7 Electrical Properties

This chapter covers the principles and applications of electrical behavior, emphasizing those related to composite materials. This includes thermoelectric behavior and the effects of temperature and stress on electrical resistivity, as well as applications such as thermoelectric energy generation, thermocouples, thermistors, heating (such as deicing), and electrical resistance-based sensing of strain, stress and damage. The materials used to make electrical connections are also covered.

7.1 Origin of Electrical Conduction

Unless noted otherwise, an electrically conductive material utilizes electrons and/or holes as the charge carriers (mobile charged particles) for electrical conduction. A hole is an electron-deficient site.

In the presence of an electric field (i.e., a voltage gradient), a hole drifts toward the negative end of the voltage gradient due to electrostatic attraction, thus resulting in a current (defined as the charge per unit time) in the same direction. In the presence of an electric field, an electron drifts toward the positive end of the voltage gradient, thus resulting in a current (defined as the charge per unit time – not the magnitude of the charge per unit time) in the opposite direction. Hence, the currents resulting from electron drift and hole drift occur in the same direction, even though electrons and holes drift in opposite directions. This means that in a material with both holes and electrons, the total current is the sum of the current due to the holes and that due to the electrons. Drift is actually a term that refers to the movement of charge in response to an applied electric field.

The drift velocity (v) is the velocity of the drift. It is actually the net velocity, since electrons or holes are quantum particles that obey the Heisenberg Uncertainty Principle, and so they constantly move, even in the absence of an applied electric field. The drift velocity is proportional to the applied electric field E, with the constant of proportionality being the mobility (μ), which describes the ease of movement of the carrier in the medium under consideration. Hence,

$$v = \mu E \,. \tag{7.1}$$

Since the units of E are V/m and the units of v are m/s, the units of μ are $m^2/(V\,s)$. For a given combination of carrier and medium, v depends on the temperature.

7.2 Volume Electrical Resistivity

The electric current (or simply "current," I, with units of ampere, or A) is defined as the charge (in coulomb, or C) flowing through the cross-section per unit time. It is the charge, not the magnitude of charge. Thus, the direction of the current is the same as the direction of positive charge flow and is opposite to the direction of negative charge flow.

The current density is the charge flow per unit cross-sectional area per unit time. The units of current density are A/m^2.

The presence of a current in a material requires the presence of charges that can move in response to the applied voltage. These mobile charges are called carriers (i.e., carriers of electricity). The carrier concentration (with units of m^{-3}) is defined as the number of carriers per unit volume.

An electrical conductor may be an electronic conductor (electrons are the main carriers), an ionic conductor (ions are the main carriers), or a mixed conductor (both ions and electrons are the main carriers). In this context, electrons constitute a class of carriers that include both electrons and holes. Holes are electron-deficient sites that are present in semiconductors and semimetals, but not in conventional metals. Holes are positively charged, since the removal of a (negatively charged) electron leaves something that is positively charged.

The current due to mobile charges with a charge q per carrier is given by

$$I = nqvA \ , \tag{7.2}$$

where n is the carrier concentration. When the carriers are electrons, $q = -1.6 \times 10^{-19}$ C. Equation 7.2 derives from the simple argument that each electron drifts by a distance v in one second, and that nvA electrons (the number of electrons in a volume of vA) move through a particular cross-section in one second, as illustrated in Fig. 7.1. Dividing Eq. 7.2 by A gives

$$I/A = nqv \ . \tag{7.3}$$

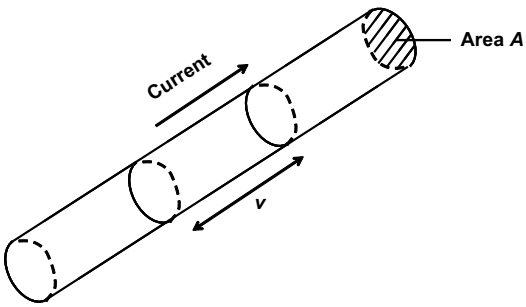

Figure 7.1. An electric current in a wire of cross-sectional area A. The current results from the drift of a type of charge carrier with a charge q per carrier at a drift velocity of v

The current density (J, with units of A/m^2) is defined as the current (I) per unit cross-sectional area (A):

$$J = I/A \ . \tag{7.4}$$

Hence, Eq. 7.3 can be written as

$$J = nqv \ . \tag{7.5}$$

Dividing Eq. 7.5 by the electric field E and using Eq. 7.1, we get

$$J/E = nq\mu \ . \tag{7.6}$$

The electrical conductivity (σ) is defined as J/E. In other words, it is defined as the current density per unit electric field. Hence, Eq. 7.6 becomes

$$\sigma = nq\mu \ . \tag{7.7}$$

From Eq. 7.7, the units of σ are $1/(\Omega\,\mathrm{m})$, i.e., $\Omega^{-1}\,\mathrm{m}^{-1}$, since the units of n are m^{-3}, the units of q are C (coulomb), and the units of μ are $\mathrm{m}^2/(\mathrm{V\,s})$. Alternate units for σ are $\mathrm{S\,m}^{-1}$, where S (short for siemens) equals Ω^{-1}. Note that, by definition,

$$\text{ampere} = \text{coulomb/second} \tag{7.8}$$

and, from Ohm's law,

$$\Omega = \text{volt/ampere} \ . \tag{7.9}$$

The electrical resistivity (ϱ) is defined as $1/\sigma$. Hence, the units of ϱ are $\Omega\,\mathrm{m}$. The electrical resistivity is also known as the volume electrical resistivity in order to emphasize that it relates to the property of a volume of the material. It is also known as the specific resistance.

The electrical resistivity ϱ is related to the electrical resistance (R) by the equation

$$R = \varrho l/A \ , \tag{7.10}$$

where l is the length of the material in the direction of the current. This length is perpendicular to the cross-sectional area A. Equation 7.10 means that the resistance R depends on the geometry such that it is proportional to l and inversely proportional to A. On the other hand, the resistivity ϱ is independent of the geometry and is thus a material property. Similarly, σ is a material property. Equation 7.7 allows the calculation of σ from n, q and μ.

The rearrangement of Eq. 7.10 gives

$$\varrho = RA/l \ . \tag{7.11}$$

Hence,

$$\sigma = l/RA \ . \tag{7.12}$$

Since, by definition, $\sigma = J/E$,

$$J/E = l/RA \ . \tag{7.13}$$

Based on Eq. 7.4, Eq. 7.13 becomes

$$I/E = l/R \ . \tag{7.14}$$

Since, by definition, $E = V/l$, Eq. 7.14 becomes

$$V = IR \ , \tag{7.15}$$

which is known as Ohm's law. Thus, the equation $\sigma = J/E$ is the same as Ohm's law.

7.3 Calculating the Volume Electrical Resistivity of a Composite Material

The volume electrical resistivity of a composite material can be calculated from the resistivities and volume fractions of all of the components. Various mathematical models are available for this calculation. The simplest model is known as the rule of mixtures (ROM), as described below for two configurations: the parallel configuration (each component is continuous and oriented in the direction of the current) and the series configuration (each component is continuous and oriented in the direction perpendicular to the current).

7.3.1 Parallel Configuration

Consider an electric current I flowing in a composite material under a voltage difference of V over a distance of l, such that the composite material consists of two components, labeled 1 and 2, as illustrated in Fig. 5.16a. The cross-sectional areas are A_1 and A_2 for Component 1 (all the strips of Component 1 together) and Component 2 (all the strips of Component 2 together), respectively. The electrical resistivities are ϱ_1 and ϱ_2 for Components 1 and 2, respectively. The current (i.e., the charge per unit time) I through the composite is given by

$$I = I_1 + I_2 \ , \tag{7.16}$$

where I_1 is the current in Component 1 (all the strips of Component 1 together) and I_2 is the current in Component 2 (all the strips of Component 2 together). Using Ohm's law,

$$I_1 = V/R_1 \tag{7.17}$$

and

$$I_2 = V/R_2 \,, \tag{7.18}$$

where R_1 is the resistance of Component 1 (all the strips of Component 1 together) and R_2 is the resistance of Component 2 (all the strips of Component 2 together). Hence, Eq. 7.16 becomes

$$I = V\left[(1/R_1) + (1/R_2)\right] \,. \tag{7.19}$$

Based on Eq. 7.10,

$$R_1 = \varrho_1 l/A_1 \,, \tag{7.20}$$

and

$$R_2 = \varrho_2 l/A_2 \,. \tag{7.21}$$

Based on Eqs. 7.20 and 7.21, Eq. 7.19 becomes

$$I = (V/l)\left[(A_1/\varrho_1) + (A_2/\varrho_2)\right] \,. \tag{7.22}$$

On the other hand, from Ohm's law,

$$I = V/R \,, \tag{7.23}$$

where R is the resistance of the composite. Based on Eq. 7.10, R is given by

$$R = \varrho l/A \,, \tag{7.24}$$

where ϱ is the resistivity of the composite and A is the total cross-sectional area of the composite. Combining Eqs. 7.23 and 7.24 gives

$$I = VA/\varrho l \,. \tag{7.25}$$

Combining Eqs. 7.22 and 7.25 gives

$$VA/\varrho l = (V/l)\left[(A_1/\varrho_1) + (A_2/\varrho_2)\right] \,, \tag{7.26}$$

or

$$A/\varrho = \left[(A_1/\varrho_1) + (A_2/\varrho_2)\right] \,. \tag{7.27}$$

Dividing by A gives

$$1/\varrho = (A_1/A)(1/\varrho_1) + (A_2/A)(1/\varrho_2) = v_1/\varrho_1 + v_2/\varrho_2 \,, \tag{7.28}$$

where v_1 and v_2 are the volume fractions of Components 1 and 2, respectively. Equation 7.28 implies that, for the parallel configuration, the reciprocal of the resistivity of the composite is the weighted average of the reciprocal of the resistivities of the two components, where the weighting factors are the volume fractions of the two components. In other words,

$$\sigma = v_1\sigma_1 + v_2\sigma_2 \,, \tag{7.29}$$

where σ is the electrical conductivity of the composite material, and σ_1 and σ_2 are the conductivities of Components 1 and 2, respectively. Equation 7.29 is a manifestation of the rule of mixtures.

Example Problem

1. Calculate the volume electrical resistivity of a composite material consisting of three components that are in parallel electrically. The resistivity required is the resistivity in the direction in which the components are parallel. Component 1 has a volume electrical resistivity of $1.4 \times 10^{-3}\,\Omega\,\text{cm}$ and a volume fraction of 0.35. Component 2 has a volume electrical resistivity of $4.4 \times 10^{-4}\,\Omega\,\text{cm}$ and a volume fraction of 0.25. Component 3 has a volume electrical resistivity of $9.5 \times 10^{-4}\,\Omega\,\text{cm}$ and a volume fraction of 0.40.

Solution:
From Eq. 7.28,

$$\begin{aligned}
1/\text{resistivity } T &= 0.35/(1.4 \times 10^{-3}\,\Omega\,\text{cm}) + 0.25/(4.4 \times 10{-}4\,\Omega\,\text{cm}) \\
&\quad + 0.40/(9.5 \times 10^{-4}\,\Omega\,\text{cm}) \\
&= 1.24 \times 10^{3}\,(\Omega\,\text{cm})^{-1}, \\
\text{Resistivity} &= 8.1 \times 10^{-4}\,\Omega\,\text{cm}\,.
\end{aligned}$$

7.3.2 Series Configuration

Consider an electric current I flowing in a composite material under a voltage difference of V over a distance of l, such that the composite material consists of two components, labeled 1 and 2, as illustrated in Fig. 7.2b. The lengths are l_1 and l_2 for Component 1 (all the strips of Component 1 together) and Component 2 (all

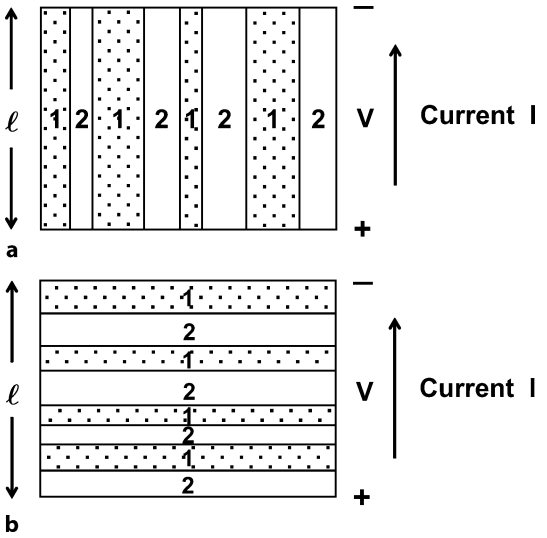

Figure 7.2. An electrically conducting composite material. The composite consists of Component 1 (*dotted regions*) and Component 2 (*white regions*). **a** Components 1 and 2 of the composite in parallel, **b** components 1 and 2 of the composite in series

the strips of Component 2 together), respectively. The electrical resistivities are ρ_1 and ρ_2 for Components 1 and 2, respectively.

The voltage drop V is given by

$$V = V_1 + V_2 \,, \tag{7.30}$$

where V_1 is the voltage drop in Component 1 (all the strips of Component 1 together) and V_2 is the voltage drop in Component 2 (all the strips of Component 2 together). From Ohm's law, and using the fact that the two components have the same cross-sectional area A and the same current I,

$$V = IR = I\rho l/A \,, \tag{7.31}$$

$$V_1 = IR_1 = I\rho_1 l_1/A \,, \tag{7.32}$$

and

$$V_2 = IR_2 = I\rho_2 l_2/A \,. \tag{7.33}$$

Combining Eqs. 7.30, 7.31, 7.32 and 7.33 gives

$$I\rho l/A = I\rho_1 l_1/A + I\rho_2 l_2/A \,, \tag{7.34}$$

or

$$\rho l = \rho_1 l_1 + \rho_2 l_2 \,. \tag{7.35}$$

Dividing by l gives

$$\rho = \rho_1(l_1/l) + \rho_2(l_2/l) = \rho_1 v_1 + \rho_2 v_2 \,, \tag{7.36}$$

where v_1 and v_2 are the volume fractions of Components 1 and 2, respectively. Equation 7.36 implies that, for the series configuration, the resistivity of the composite material is the weighted average of the resistivities of the two components, where the weighting factors are the volume fractions of the two components. Equation 7.36 is a manifestation of the rule of mixtures.

7.4 Contact Electrical Resistivity

An interface is associated with an electrical resistance in the direction perpendicular to the interface. The contact electrical resistance refers to the resistance of an interface between two objects (or between two components in a composite material) when a current is passed across the interface in the direction perpendicular to the interface. When the interface has air voids, for example, the contact resistance will be relatively high. This is because air is an electrical insulator and the objects themselves are more conductive than air. When the interface has an impurity that is less conductive than the objects themselves, the contact resistance will also be

relatively high. Thus, the contact resistance is highly sensitive to the condition of the interface.

The contact resistance also depends on the area of the interface. The larger the area, the lower the contact resistance. Hence, the contact resistance R_c is inversely proportional to the interface area A, and the relationship between these two quantities can be written as

$$R_c = \rho_c / A \ , \tag{7.37}$$

where the proportionality constant ρ_c is known as the contact electrical resistivity. This quantity does not depend on the area of the interface; it only reflects the condition of the interface. The units of ρ_c are $\Omega\,\mathrm{cm}^2$, which are different from those of the volume resistivity ρ, $\Omega\,\mathrm{cm}$.

7.5 Electric Power and Resistance Heating

7.5.1 Scientific Basis

The electric power P associated with the flow of a current I under a voltage difference V is given by

$$P = VI \ . \tag{7.38}$$

This power is dissipated as heat, thus allowing a form of heating known as resistance heating. Applications of this include the deicing of aircraft and bridges. This effect, in which electrical energy is converted to thermal energy, is known as the Joule effect. The units of P are watts (W), with watt = volt $\times$ ampere. Based on Eq. 7.15, Eq. 7.38 can be expressed as

$$P = I^2 R \tag{7.39}$$

and as

$$P = V^2 / R \ . \tag{7.40}$$

Therefore, in order to obtain a high value for the power, both V and I should not be too small (Eq. 7.38). The values of V and I depend on the resistance R. When R is small, V is small since $V = IR$. When R is large, I is small since $I = V/R$. Thus, an intermediate value of R is optimal for obtaining a high power. It is R rather ρ that governs P. Therefore, for a given material (i.e., a given value of ρ), the dimensions can be chosen to obtain a particular value of R (Eq. 7.10). Since the current direction does not affect the resistance heating, the heating can be carried out using DC or AC electricity.

Consider an example in which $R = 1\,\mathrm{M}\Omega$ (i.e., $10^6\,\Omega$) and $V = 120\,\mathrm{V}$ (which is a common voltage from an electrical outlet). Hence,

$$I = V/R = (120\,\mathrm{V})/(1 \times 10^6\,\Omega) = 1.2 \times 10^{-4}\,\mathrm{A} = 0.12\,\mathrm{mA} \ , \tag{7.41}$$

and

$$P = VI = (120\,\mathrm{V})(1.2 \times 10^{-4}\,\mathrm{A}) = 1.4 \times 10^{-2}\,\mathrm{W} = 14\,\mathrm{mW}\,. \tag{7.42}$$

Consider another example in which $R = 1\,\mathrm{k}\Omega$ (i.e., $1 \times 10^3\,\Omega$) and $V = 120\,\mathrm{V}$. Hence,

$$I = V/R = (120\,\mathrm{V})/(1 \times 10^3\,\Omega) = 0.12\,\mathrm{A}\,, \tag{7.43}$$

and

$$P = VI = (120\,\mathrm{V})(0.12\,\mathrm{A}) = 14\,\mathrm{W}\,. \tag{7.44}$$

Now consider another example in which $R = 1\,\Omega$ and $V = 120\,\mathrm{V}$. Hence,

$$I = V/R = (120\,\mathrm{V})/(1\,\Omega) = 120\,\mathrm{A}\,, \tag{7.45}$$

which is a current that is too high to be provided by conventional power sources, which often limit the current to, say, 1 A. Thus, in spite of the high V that the power source can provide, the actual V across the heating element is just

$$V = IR = (1\,\mathrm{A})(1\,\Omega) = 1\,\mathrm{V}\,, \tag{7.46}$$

and the power is thus merely

$$P = VI = (1\,\mathrm{V})(1\,\mathrm{A}) = 1\,\mathrm{W}\,. \tag{7.47}$$

Therefore, among the three examples mentioned above, the intermediate R of $1\,\mathrm{k}\Omega$ gives the highest P.

Nichrome (Ni-20Cr alloy), with $\rho = 1 \times 10^{-4}\,\Omega\,\mathrm{cm}$, is a material that is commonly used for resistance heating because it has a relatively high resistivity for a metal. We can calculate the length of the wire required for a nichrome wire of diameter 1 mm to provide a resistance of $1\,\mathrm{k}\Omega$ using Eq. 7.10:

$$l = RA/\rho = (1\,\mathrm{k}\Omega)\left[\pi(0.5\,\mathrm{mm})^2\right]/(1 \times 10^{-4}\,\Omega\,\mathrm{cm}) = 7.9 \times 10^4\,\mathrm{cm} = 790\,\mathrm{m}\,. \tag{7.48}$$

This length of 790 m is quite long, so the wire cannot be packaged linearly; it needs to be coiled. This is why heating elements commonly take the form of coils.

In order to pass current to a heating element, two electrical contacts are required, as illustrated in Fig. 7.3. An electrical contact may, for example, be a soldered joint

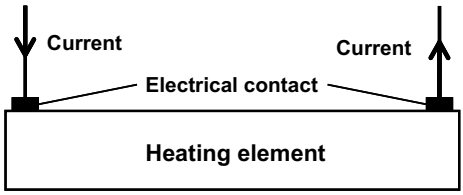

Figure 7.3. Electrical contacts that are used to pass current to a heating element contribute to the electrical resistance

between the heating element and a wire. Each electrical contact is associated with a resistance, which is the sum of (i) the resistance of the joining medium (e.g., solder), (ii) the resistance of the interface between the joining medium and the heating element, and (iii) the resistance of the interface between the joining medium and the wire. Since the joining medium is typically a highly conductive material, the resistance of the joining medium is usually negligible compared to the two interfacial resistances. The interfacial resistance can be substantial due to air voids, impurities, reaction products or other species at the interface. The resistances of both of the contacts contribute to the resistance R encountered by the current I. Therefore, the design of a heating element must consider the contribution to R from the electrical contacts. In particular, the resistance from the two contacts must not be so large that it overshadows the resistance within the heating element material. If it is too large, the electrical contacts become the main heating elements, while the actual heating element contributes little to heat generation, resulting in nonuniform heating as it is concentrated at the electrical contacts.

7.5.2 Self-Heating Structural Materials

7.5.2.1 Introduction

Resistance heating (or Joule heating) involves the conversion of electricity into heat. It requires a heating element through which electric current is passed. Heating elements are commonly used in toasters and hair dryers. Other applications include deicing, home improvement, ovens, space heating, warming vests, heating pads, electric blankets, and seat heating.

The materials most commonly used for heating elements are metal alloys, such as nichrome (an alloy with a common composition of 80% nickel and 20% chromium), which is attractive due to its low cost, high resistivity (compared to many other metals), and its resistance to oxidation or degradation in air at elevated temperatures. In spite of its high resistivity compared to many metals, its resistivity is low compared to carbon or ceramics. Because of this low resistivity (typically $10^{-5}\,\Omega\,\text{cm}$), sufficient resistance in the metallic heating element is commonly attained by using a long length of the metal, which may be coiled or take the form of an etched foil or a patterned thick film. The thick film is made from a paste that contains the metal in powder form.

Compared to metals, carbon is attractive due to its higher resistivity (typically $10^{-3}\,\Omega\,\text{cm}$), high temperature resistance, ability to radiate heat, and its availability in the form of fibers. Carbon heating elements take the form of continuous carbon fiber, unwoven carbon fiber mats/felts, woven carbon fiber fabrics, and flexible graphite. Flexible graphite (also known as Grafoil) is a graphite sheet that is formed by compressing exfoliated graphite in the absence of a binder.

Heating elements that are also structural components are attractive, particularly when the heating is needed for purposes such as deicing in aeronautical and automotive systems, transportation infrastructures (e.g., aircraft, driveways, airport runways, highways and bridges), and industrial systems. This can be achieved by

incorporating a nonstructural heating element into the structural component. For example, the nonstructural heating element can take the form of a sheet that is at or near the surface of the structural component. Examples of nonstructural heating elements include flexible graphite and carbon fiber mats, which are mechanically inadequate for load bearing. An alternate method involves using the load-bearing structural material as the heating element, so that the structural material becomes multifunctional and the need to combine a structural element with a nonstructural element is eliminated. Attractions of this alternative method include higher durability (no need to worry about the detachment of the nonstructural element from the structural element, or about the possible mechanical degradation of the nonstructural element), lower fabrication cost, greater implementation convenience, higher spatial uniformity of the heating, and greater volume of the heating element. Structural materials that also function as heating elements are said to be self-heating.

The dominant structural materials in this context are cement-matrix composites (for buildings) and continuous fiber polymer–matrix composites (for lightweight structures such as aircraft). These materials cannot withstand high temperatures. However, heating to temperatures that are not far from room temperature is needed for deicing, comfortable living, and hazard mitigation. For example, in deicing, the relevant temperature is around 0°C. This section addresses self-heating in both types of structural composites.

The materials used in heating elements cannot have electrical resistivities that are too low, as this would result in the resistance of the heating element being too low and so a high current would be needed to achieve a specific power. The materials of heating elements cannot be too resistive either, as this would result in a current in the heating element that is too low (unless the voltage is very high). Materials used in heating elements include metal alloys, ceramics (such as silicon carbide), graphite, polymer–matrix composites, carbon–carbon composites, asphalt, and concrete.

Resistance heating is useful for heating buildings, for deicing bridge decks, driveways and aircraft, for plastic welding, and for the demolition of concrete structures. On the other hand, electrical self-heating is undesirable for optimizing the performance and reliability of electrical interconnections, bolometers, superconductors, transistors, diodes, and other semiconductor devices.

7.5.2.2 Self-heating Cement-Matrix Composites

Conventional concrete is electrically conductive but its resistivity is too high for resistance heating to be effective. The resistivity of concrete can be diminished by the use of electrically conductive admixtures or aggregates, such as discontinuous carbon fibers, discontinuous steel fibers or shavings, and graphite or carbon particles. It can also be diminished by using an alkaline slag binder. However, the most effective method of decreasing the resistivity is to use a conductive admixture at a volume fraction beyond the percolation threshold. Percolation means the attainment of a continuous conductive path due to contact between adjacent conductive fibers or particles. The objective of this section is to compare various conductive

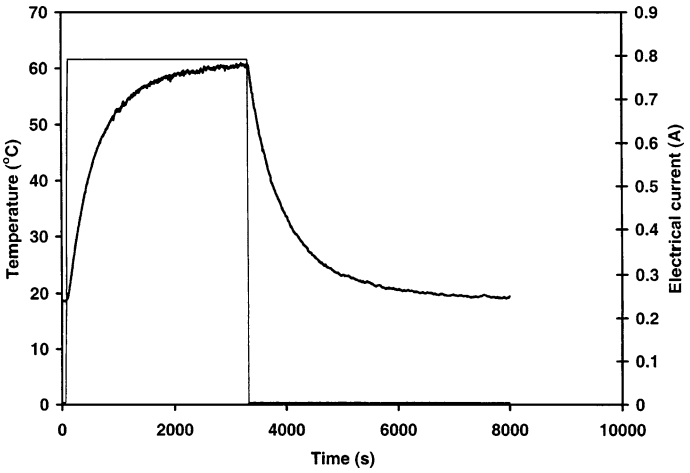

Figure 7.4. Temperature variation during heating (current on) and subsequent cooling (current off) when using steel fiber (8 µm diameter) cement as the resistance heating element. *Thick curve*: temperature, *thin curve*: current. (From [1])

cement-matrix composites in terms of resistance heating effectiveness. These composites have lower resistivities than cement itself (by orders of magnitude) due to the percolation of the conductive admixtures.

Due to the exceptionally low electrical resistivity (0.85 Ω cm) attained by ising 8 µm diameter steel fibers in cement, cement with the steel fibers is a highly effective material for heating, as described below. A DC electrical power input of 5.6 W (7.1 V, 0.79 A) results in a maximum temperature of 60°C (initial temperature = 19°C) and a time of 6 min to achieve half of the maximum temperature rise (Fig. 7.4). The efficiency of energy conversion increases with the duration of heating, reaching 100% after 50 min (Fig. 7.5). The heat power output per unit area provided by steel fiber cement is 750 W/m^2, compared to 340 W/m^2 for a metal wire with the same

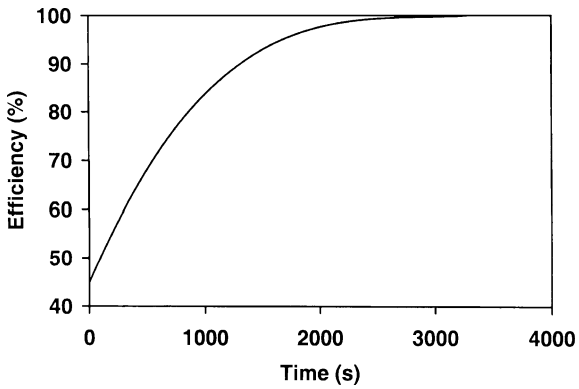

Figure 7.5. Efficiency vs. time for the heating of steel fiber (8 µm diameter) cement at a current of 0.48 A (from [1])

resistance. Due to the presence of steel fibers, the structural properties are superior to those of conventional cement-based materials.

In contrast, for carbon fiber (1.0 vol%) cement of electrical resistivity 104 Ω cm, an electrical power input of 1.8 W (28 V, 0.065 A) results in a maximum temperature of 56°C (initial temperature = 19°C) and a time of 256 s to achieve half of the maximum temperature rise. The high voltage (28 V, compared to 7 V in the case of steel fiber cement) is undesirable due to the voltage limitations of typical power supplies. The performance is even worse for graphite particle (37 vol%) cement paste of resistivity 407 Ω cm.

The steel fibers mentioned above are only 8 μm in diameter. Steel fibers of larger diameter (e.g., 60 μm) are much less effective at reducing the electrical resistivities of cement-based materials and are therefore less effective for self-heating. For example, cement paste with 8 μm diameter steel fibers at 0.54 vol% gave a resistivity of 23 Ω cm, whereas steel fibers of 60 μm diameter at 0.50 vol% led to resistivity 1.4×10^3 Ω cm, steel fibers of 8 μm diameter at 0.36 vol% gave a resistivity of 57 Ω cm, and steel fibers of 60 μm diameter at 0.40 vol% gave a resistivity of 1.7×10^3 Ω cm.

An alternative concrete technology involves using steel shavings (0.15–4.75 mm in particle size) as the conductive aggregate in conjunction with low-carbon steel fibers as the conductive admixture. The use of 20 vol% steel shavings together with 1.5 vol% steel fibers resulted in an electrical resistivity of 75–100 Ω cm. The resistivity increased over time, reaching 350 Ω cm in six months, presumably due to the corrosion of the steel shavings and fibers. The high resistivity and the increase in resistivity with time are undesirable. In contrast, cement with stainless steel fibers (8 μm diameter, 0.7 vol%) has a low resistivity of 0.85 Ω cm and the resistivity is stable over time. Furthermore, it does not require any special mixing equipment or procedure and does not require any special aggregate.

7.5.2.3 Self-heating Polymer-Matrix Composites

Self-heating in continuous fiber polymer-matrix composites can be attained using the following methods: (a) by embedding a low-resistivity interlayer (e.g., a carbon fiber mat) between adjacent laminae during composite fabrication and using the interlayer as a heating element, (b) by using conductive reinforcing fibers (e.g., continuous carbon fibers) to make the composite conductive and using the overall composite as a heating element, and (c) by using the interlaminar interface between adjacent laminae of conductive reinforcing fibers (e.g., continuous carbon fibers) as a heating element.

Method (a) is the one most commonly employed, as it is applicable to a broad range of composites, whether the reinforcing fibers are conductive or not. Method (b) is also feasible, but suffers from difficulties in attaining localized heating. Method (c) involves an innovative concept in which the contact resistance associated with the interlaminar interface between laminae of conductive fibers allows the interface to serve as a heating element. The interface between two crossply laminae can be subdivided to provide a two-dimensional array of heating elements, in addition to an x–y grid of electrical interconnections, thereby allowing spatially distributed heating (Fig. 7.6) and a very small thermal mass for each

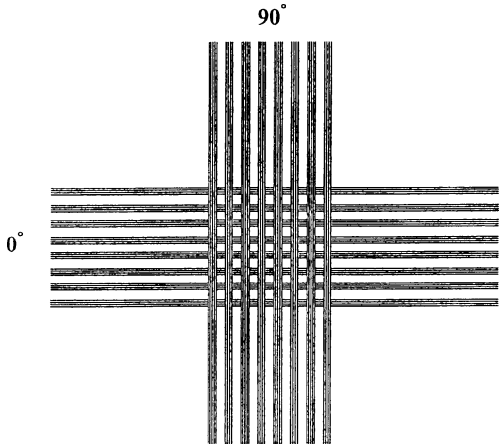

Figure 7.6. Sensor array in the form of a carbon fiber polymer-matrix composite comprising two crossply laminae (from [2])

heating element. Figure 7.7 shows the ability of the interlaminar interface to serve as a resistance heating element. The area of the interface is 5×5 mm and there is a resistance of 0.067 Ω in the direction perpendicular to the area. The heat power output is up to 4×10^4 W/m^2.

An example of the application of method (a) involves the use of a porous mat comprising short carbon fibers and a small proportion of an organic binder as the interlayer. The fibers in a mat are randomly oriented in two dimensions. The mats are made by wet-forming, as in papermaking. A mat comprising bare short carbon fibers and exhibiting a volume electrical resistivity of 0.11 Ω cm and a thermal stability of up to 205°C has been shown to be effective as a resistive heating element. It provides temperatures of up to 134°C (initial temperature = 19°C) at a power of up to 6.5 , with a time of up to 106 s required to achieve half of the

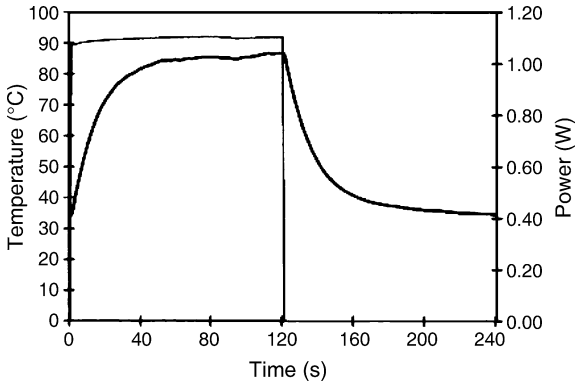

Figure 7.7. The interlaminar interface of a crossply two-lamina carbon fiber epoxy-matrix composite serving as a resistance heating element. The temperature rises while the power is applied and drops during the subsequent period when it is not. *Thick curve*: temperature, *thin curve*: power. (From [2])

maximum temperature rise. The electrical energy used to increase the temperature by 1°C during the initial rapid temperature rise (5 s) is up to 3.8 J. The efficiency is nearly 1.00, even in the first 5 s of heating. A mat comprising metal (Ni/Cu/Ni trilayer)-coated short carbon fibers and exhibiting a volume electrical resistivity of 0.07 Ω cm provides lower temperatures (up to 79°C) but a faster response (up to 14 s to achieve half of the maximum temperature rise).

An example of the application of method (c) involves the use of the interface between two crossply laminae of a continuous carbon fiber epoxy-matrix composite. For an interface of area 5 × 5 mm and a resistance of 0.067 Ω, a DC electrical power input of 0.59 W (3.0 A, 0.20 V) results in a maximum temperature of 89°C (initial temperature = 19°C). The time needed to reach half of the maximum temperature rise is up to 16 s. The efficiency of energy conversion reaches 100% after about 55 s of heating, when the heat power output is up to 4×10^4 W/m^2 of the interlaminar interface.

7.5.2.4 Comparison of Self-heating Structural Materials

Table 7.1 shows a comparison of various materials in terms of their self-heating effectiveness, as evaluated in the laboratory of the author. The carbon fiber epoxy-matrix interlaminar interface (No. 6 in Table 7.1) and the Ni/Cu/Ni-coated carbon fiber mat (No. 5 in Table7.1) have exceptional abilities to provide fast and significant temperature responses, though they have low power capacities. Carbon fiber mat (No. 4 in Table 7.1) has an exceptional ability to deliver high power and significant temperature rises; it is superior to cement-matrix composites (Nos. 1–3 in Table 7.1) in terms of power capacity, temperature capacity, and fast response. On the other hand, it is much inferior to flexible graphite (not a structural material; No. 7 in Table 7.1) in terms of all three attributes.

A comparison of the volume electrical resistivities of the various materials in Table 7.1 shows that a low resistivity tends to be associated with good self-heating performance, although there are exceptions. The outstanding performance of flexible graphite is attributed to its outstandingly low resistivity.

The maximum temperature is limited by the ability of the material to withstand high temperatures. Flexible graphite is outstanding in this ability. However, the maximum temperature is also determined by the ability of the material to sustain current. A low resistivity greatly helps this ability, as shown by comparing the performances of the three cement-based materials (Nos. 1–3 in Table 7.1).

The time to reach half of the maximum temperature rise increases with the maximum temperature rise, as shown by comparing the response times at different input powers for the same material. This time is expected to be reduced by a decrease in thermal mass (which relates to the mass and the specific heat) or an increase in thermal conductivity. The fast response of the carbon fiber epoxy-matrix interlaminar interface is attributed mainly to its low thermal mass, which is due to the microscopic thickness of the interface. The fast responses of the Ni/Cu/Ni-coated carbon fiber mat and the flexible graphite are attributed mainly to the high thermal conductivity.

Table 7.1. Effectiveness of self-heating from a temperature of 19°C

Material	Maximum temperature (°C)	Time to reach half of the maximum temperature rise	Power (W)	Volume resistivity (Ω cm)
1. Steel fiber (0.7 vol%) cement	60	6 min	5.6	0.85
2. Carbon fiber (1.0 vol%) cement	56	4 min	1.8	100
3. Graphite particle (37 vol%) cement	24	4 min	0.27	410
4. Carbon fiber (uncoated) mat	134	2 min	6.5	0.11
5. Ni/Cu/Ni-coated carbon fiber mat	79	14 s	3.0	0.07
6. Carbon fiber epoxy-matrix interlaminar interface	89	16 s	0.59	–[b]
7. Flexible graphite[a]	980	4 s	94	7.5×10^{-4}

[a] Not a structural material
[b] The relevant quantity is the contact resistivity rather than the volume resistivity

The power in Table 7.1 is the electrical power input, which is essentially equal to the heat power output after an initial period in which the material itself is being heated. The power is governed by the ability of the material to sustain current and voltage. This ability is enhanced by a decrease in resistivity.

Although the resistivity is not the only criterion that governs the effectiveness of a material for self-heating, it is the dominant criterion, particularly in relation to the power and the maximum temperature. In general, the selection of a self-heating structural material depends on the requirements in terms of the maximum temperature, the power response time, and the mechanical properties. For cement-based structures, steel fiber cement (No. 1 in Table 7.1) is recommended. For a continuous fiber polymer–matrix composite, carbon fiber mat (No. 4 in Table 7.1) is recommended for use as an interlayer. For spatially distributed heating, the carbon fiber epoxy-matrix interlaminar interface is recommended.

Flexible graphite cannot be incorporated into a structural composite due to its mechanical weakness and impermeability to resin. However, it can be placed on a structural material, and its flexibility allows it to conform to the topography of the structural material.

7.5.2.5 Summary of Self-heating Structural Materials

Self-heating structural materials in the form of cement-matrix and polymer–matrix composites have been engineered by using electrically conductive fibers (continuous or discontinuous) and interlayers. Both the volume of the composite and the interlaminar interface can be used as heating elements. The interlaminar

interface between continuous carbon fiber laminae is attractive since it is amenable to providing a two-dimensional array of heating elements. A cement-matrix composite containing 0.7 vol% steel fibers (8 μm diameter) and a mat of discontinuous uncoated carbon fibers for use as an interlayer are effective for self-heating. However, the effectiveness of such a system is low compared to flexible graphite, which is not a structural material.

7.6 Effect of Temperature on the Electrical Resistivity

7.6.1 Scientific Basis

For a given material, the volume electrical resistivity depends on the temperature. This dependence means that the resistivity can be employed as an indicator of the temperature; in other words, by measuring the resistance, one can obtain the temperature. This type of temperature sensor is known as a thermistor.

The dependence of the volume electrical resistivity on temperature is expressed by the temperature coefficient of electrical resistivity (α), which is defined as

$$(\Delta\rho)/\rho_o = \alpha\Delta T \,, \tag{7.49}$$

where ρ_o is the resistivity at 20°C and $\Delta\rho$ is the change in resistivity relative to ρ_o when the temperature is increased or decreased from 20°C by ΔT. The units of α are $°C^{-1}$. Since

$$\Delta\rho = \rho - \rho_o \,, \tag{7.50}$$

Equation 7.49 can be rewritten as

$$\rho = \rho_o(1 + \alpha\Delta T) \,. \tag{7.51}$$

Thus, the plot of ρ vs. ΔT gives a line with a slope of $\rho_o\alpha$. This line tends to be straight only for metals. However, temperature sensing based on this phenomenon does not require the curve to be a straight line. The greater the magnitude of α, the more sensitive the thermistor.

For metals, α is positive; in other words, the resistivity increases with increasing temperature. This is because the amplitudes of the thermal vibrations of the atoms in the metal increase with increasing temperature, thereby decreasing the mobility μ (as defined in Eq. 7.1). A decrease in mobility in turn results in a decrease in the conductivity (Eq. 7.7); in other words, an increase in the resistivity. The carrier concentration n of a metal does not change with temperature, due to the availability of the valence electrons as mobile charges without any need to excite them. When the temperature is 0 K, there is no thermal energy to provide thermal vibrations, so the resistivity at this temperature is not due to thermal vibrations but rather the scattering of the electrons (carriers) at any defects present in the material. The resistivity at 0 K is known as the residual resistivity (Fig. 7.8). The greater the defect concentration, the higher the residual resistivity.

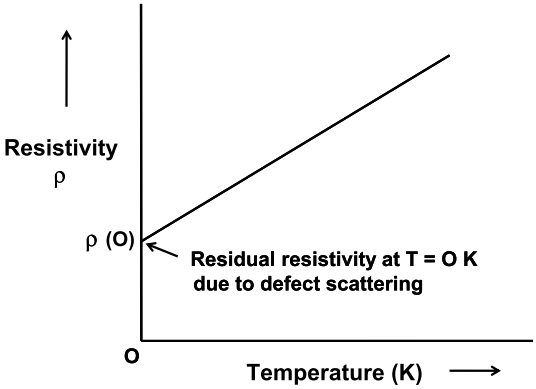

Figure 7.8. Dependence of the volume electrical resistivity on the temperature near 0 K, showing the residual resistivity at 0 K

Semiconductors (e.g., silicon and germanium) and semimetals (e.g., graphite) together constitute a class of materials known as metalloids (or semimetals). For metalloids, α is negative. This is because, for these materials, n increases significantly with increasing temperature. This trend in n is due to the thermal excitation of electrons to form mobile carriers. For a semiconductor, the valence electrons need to be excited across the energy band gap in order for them to become mobile. The larger the energy band gap, the greater the effect of temperature on the resistivity. For a semimetal there is no energy band gap, only a small band overlap, thus resulting in a small effect of temperature on the resistivity. The increase in n with increasing temperature predominates over the decrease in mobility μ with increasing temperature (Eq. 7.7), thus resulting in an overall effect in which the conductivity increases with increasing temperature (i.e., the resistivity decreases with increasing temperature).

For metals, the value of α is typically around +0.004/°C. For semiconductors and semimetals, α is negative, but its magnitude is higher for semiconductors than for semimetals due to the energy band gap present in a semiconductor. Thus, the magnitude of α is smaller for carbon (a semimetal) than for silicon or germanium (semiconductors). The magnitude of α is larger for silicon than germanium due to the larger energy band gap for silicon (1.12 eV, compared to 0.68 eV for germanium). The energy band gap (also known as the energy gap) is the energy between the top of the valance band and the bottom of the conduction band above the valence band, and describes the energy needed to excite an electron from the valence band to the conduction band so that the electron becomes free to respond to an applied electric field.

For a composite with an electrically nonconductive matrix and a conductive discontinuous filler (particles or fibers) where the CTE of the matrix is higher than that of the filler, increasing the temperature causes more thermal expansion of the matrix than the filler. As a consequence, the degree of contact between adjacent filler units (i.e., adjacent particles or adjacent fibers) is reduced, causing the volume resistivity of the composite to increase. The resistivity typically increases abruptly

when the increase in temperature has reached a sufficiently large value. This means that the curve of resistivity vs. temperature is not linear. When the filler volume fraction is around the percolation threshold, the increase in resistivity is particularly large. This is because the resistivity is particularly sensitive to the degree of contact between adjacent filler units when the filler volume fraction is around the percolation threshold. This phenomenon is useful for temperature-activated switching – the deactivation of a circuit (due to the high resistivity of the composite used in series in the circuit) when the temperature is higher than a critical value. The composite therefore serves as a fuse that protects the electronics from excessive temperatures.

7.6.2 Structural Materials Used as Thermistors

7.6.2.1 Polymer-Matrix Structural Composites Used as Thermistors and Thermal Damage Sensors

Continuous fiber polymer-matrix composites are structural composites, in contrast to the relative weaknesses of short-fiber polymer-matrix composites. The interlaminar interface of a continuous carbon fiber polymer-matrix composite is associated with a contact (two-dimensional) resistivity that decreases quite reversibly upon heating, as shown in Fig. 7.9, thereby allowing it to be a thermistor. The contact resistivity of the interface decreases with increasing temperature because of the energy needed for electrons to jump from one lamina to the next through the interlaminar interface. The higher the temperature, the greater the thermal energy available, and the larger the proportion of electrons that manage to jump across the interface. By using the configuration shown in Fig. 7.6, one can

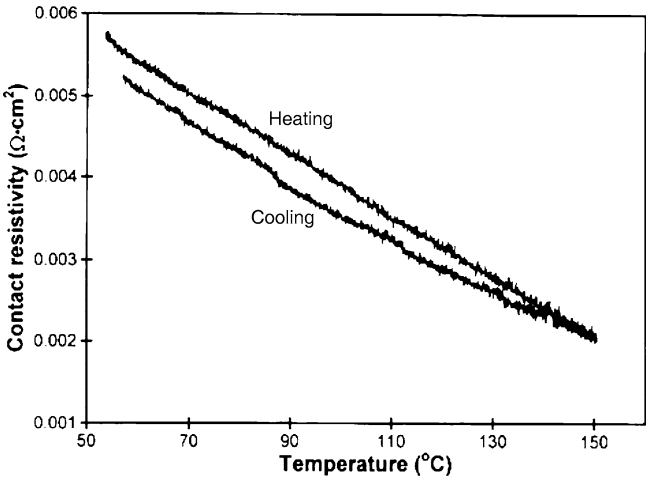

Figure 7.9. Variation in the contact electrical resistivity with temperature during heating and cooling at 0.15°C/min of the crossply interlaminar interface of a continuous carbon fiber epoxy-matrix composite made with a curing pressure of 0.33 MPa (from [3])

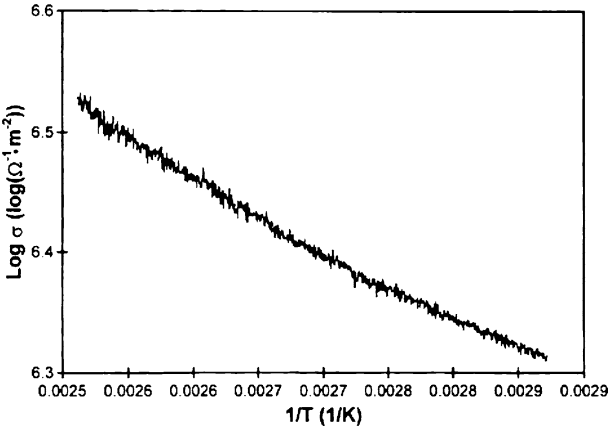

Figure 7.10. Arrhenius plot of log contact conductivity versus inverse absolute temperature during heating at 0.15°C/min for the crossply interlaminar interface of a continuous carbon fiber epoxy-matrix composite made with a curing pressure of 0.33 MPa (from [3])

obtain a two-dimensional array of thermistors, thereby enabling spatially resolved temperature sensing.

Corresponding Arrhenius plots of log contact conductivity (inverse of contact resistivity) versus inverse absolute temperature during heating are shown in Fig. 7.10. From the slope (negative) of the Arrhenius plot, which is quite linear, the activation energy can be calculated by using the equation

$$\text{Slope} = -E/(2.3\,k_B)\,, \tag{7.52}$$

where k_B is the Boltzmann constant, T is the absolute temperature (in K) and E is the activation energy, which is thus found to be 0.118 eV. This activation energy is the energy needed for an electron to jump from one lamina to the next. Exciting electrons to this energy enables conduction in the through-thickness direction.

Figure 7.11 shows the sensing of both temperature and thermal damage through the measurement of the contact electrical resistivity (the geometry-independent quantity equal to the product of the contact resistance and the contact area) of the interlaminar interface. The resistivity decreases upon heating during each heating cycle due to the activation energy associated with the movement of electrons across the interface. This is the thermistor effect, which allows temperature sensing. Minor thermal damage at the maximum temperature of the hottest cycle causes a spike in the resistivity, allowing damage sensing.

Polymer-matrix composites with conductive short fibers or particles can also function as thermistors, due to the increase in spacing between adjacent filler units as the polymer matrix (which has a high CTE compared to the filler) expands upon heating. The increase in spacing means that the chance of filler units touching one another to form a continuous conductive path is decreased, thereby causing the resistivity of the composite to increase. Instead of increasing smoothly with increasing temperature, the resistivity tends to increase abruptly as the temperature

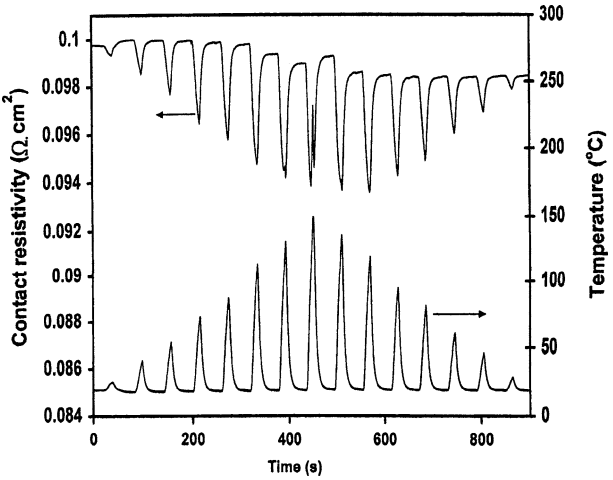

Figure 7.11. The contact electrical resistivity of the interlaminar interface of a crossply continuous carbon fiber epoxy-matrix composite during temperature variation (from [3])

increases beyond a certain level. As a result, the resistance of such a composite is not a very good indicator of the temperature.

7.6.2.2 Cement-Matrix Structural Composites Used as Thermistors and Freeze–Thaw Damage Sensors

Cement is a material that is slightly conductive, with both ions and electrons involved in the conduction. The volume electrical resistivity of cement paste is around $10^5\,\Omega\,\text{cm}$, as compared to $10^{-3}\,\Omega\,\text{cm}$ for carbon and $10^{-6}\,\Omega\,\text{cm}$ for copper. This resistivity decreases with increasing temperature because of the inhomogeneity of cement paste and the thermally activated jumping of carriers across the diffuse interfaces associated with this inhomogeneity. The inhomogeneity stems from the incomplete curing of some of the cement particles and the partial setting or curing of some of the cement particles prior to their incorporation in the cement mix. The sensitivity of a cement-based thermistor is enhanced by the addition of short carbon fiber, which introduces fiber–cement interfaces and decreases the resistivity of the composite. Figure 7.12 shows the decrease in the volume electrical resistivity of carbon-fiber (short) silica-fume cement paste with increasing temperature. The fiber volume fraction is below the percolation threshold (i.e., the fibers do not touch one another sufficiently to form a continuous conductive path in the composite). The resistivity is $2 \times 10^4\,\Omega\,\text{cm}$, compared to $6 \times 10^5\,\Omega\,\text{cm}$ for silica-fume cement (without fiber) and $5 \times 10^5\,\Omega\,\text{cm}$ for plain cement paste (without silica fume or fiber). Figure 7.13 shows the corresponding Arrhenius plot, the slope of which gives the activation energy of the conduction. The activation energy is 0.390 eV, compared to 0.035 eV for silica-fume cement paste and 0.040 eV for plain cement paste. The activation energy is much higher in the presence of carbon fiber.

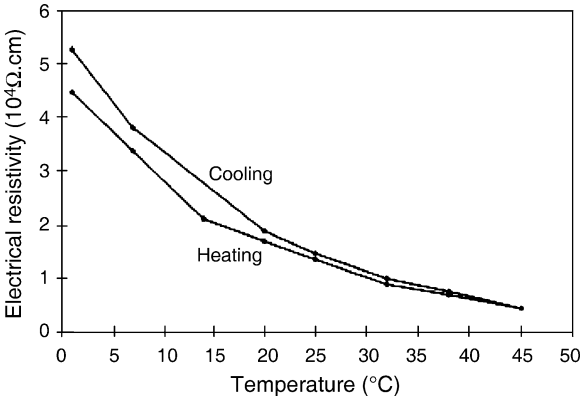

Figure 7.12. Plot of electrical resistivity vs. temperature during heating and subsequent cooling for carbon fiber silica fume cement paste (from [4])

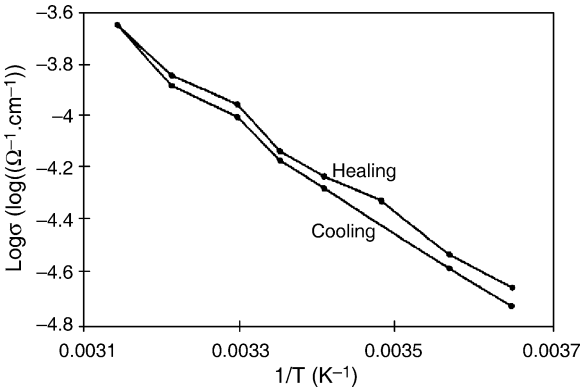

Figure 7.13. Arrhenius plot of log electrical conductivity vs. reciprocal absolute temperature for carbon-fiber silica-fume cement paste (from [4])

Damage causes the volume resistivity to increase irreversibly, while increasing the temperature in the absence of damage causes the resistivity to decrease reversibly. A common cause of damage in cement-based materials is freeze–thaw cycling, which is detrimental to the integrity of the material. The mechanism of the damage involves the expansion of the water present in the pores of a cement-based material upon freezing. The progression of freeze–thaw damage can be monitored by measuring the volume resistivity of the cement-based material while the temperature is simultaneously monitored. This monitoring is feasible even in the absence of a conductive admixture such as carbon fibers. As shown in Fig. 7.14 for cement mortar, the resistivity decreases upon cooling during each temperature cycle due to the activation energy associated with charge carrier movement in the cement-based material. This effect of temperature allows the cement-based material to function as a thermistor for temperature sensing. At the end of each freeze–thaw cycle, the resistivity is slightly higher than the value at the beginning

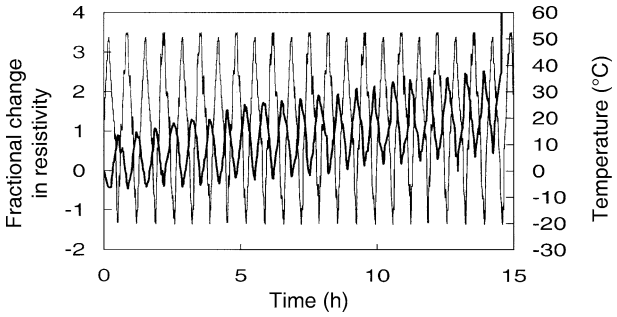

Figure 7.14. Variation in the volume electrical resistivity (fractional change) with time, and of the temperature with time, during freeze–thaw cycling of cement mortar (with fine aggregate, but without any conductive admixture). *Thick curve*: fractional change in resistivity, *thin curve*: temperature. (From [5])

of the cycle. This is due to the occurrence of minor damage during each cycle, including the first cycle. The damage accumulates cycle by cycle, as shown by the irreversible increase in the resistivity with each cycle. Failure occurs at the coldest point of the last cycle, as shown by the abrupt increase in resistance.

7.7 Effect of Strain on the Electrical Resistivity (Piezoresistivity)

7.7.1 Scientific Basis

Piezoresistivity is a phenomenon in which the electrical resistivity of a material changes with strain. It is useful from a practical point of view since it enables strain sensing through electrical resistance measurement. Strain sensing should be distinguished from damage sensing. Strain causes reversible effects, whereas damage causes irreversible effects.

The resistance R is related to the resistivity ϱ, the length ℓ in the direction of resistance measurement, and the cross-sectional area A perpendicular to the direction of resistance measurement:

$$R = \varrho\ell/A \; . \tag{7.53}$$

The fractional change in resistance is given by the equation

$$\delta R/R = \delta\varrho/\varrho + (\delta\ell/\ell)(1 - \nu_{12} - \nu_{13}) \; , \tag{7.54}$$

where ν_{12} and ν_{13} are values of the Poisson ratio for the transverse and through-thickness strains, respectively. If the material is isotropic, so that $\nu_{12} = \nu_{13} = \nu$, Eq. 7.54 becomes

$$\delta R/R = \delta\varrho/\varrho + (\delta\ell/\ell)(1 - 2\nu) \; . \tag{7.55}$$

Positive piezoresistivity refers to behavior where the resistivity increases with increasing strain, i.e., $(\delta\varrho/\varrho)/(\delta\ell/\ell) > 0$. Negative piezoresistivity refers to behavior where the resistivity decreases with increasing strain, i.e., $(\delta\varrho/\varrho)/(\delta\ell/\ell) < 0$. Piezoresistivity is usually positive, because elongation tends to change the microstructure in such a way that the resistivity increases in the direction of elongation. For example, a composite with an electrically nonconductive polymer matrix and a filler in the form of electrically conductive particles or short fibers tends to exhibit positive piezoresistivity, because the distance between adjacent particles increases upon elongation of the composite, thereby decreasing the chance of contact between the adjacent particles. However, negative piezoresistivity has been reported in polymer-matrix composites with continuous carbon fibers and with carbon nanofiber, as well as in semiconductors.

To achieve effective strain sensing, a large fractional change in resistance per unit strain is desirable. Thus, the severity of piezoresistivity is commonly described in terms of the gage factor, which is defined as the fractional change in resistance per unit strain. Equation 7.54 shows that the gage factor depends on both the fractional change in resistivity per unit strain and the Poisson ratio. A positive value of the gage factor does not necessarily mean that the piezoresistivity is positive, but a negative value of the gage factor necessarily means that the piezoresistivity is negative.

In order to attain a large fractional change in resistance at a particular strain, positive piezoresistivity is more desirable than negative piezoresistivity for the same fractional change in resistivity. When the strain is small, which is the case for example when the piezoresistive material is a stiff structural material, the fractional change in resistance is essentially equal to the fractional change in resistivity. In this case, positive and negative piezoresistivities are equally desirable for achieving a large fractional change in resistance. Note that, in terms of its scientific origin, negative piezoresistivity is more intriguing than positive piezoresistivity.

7.7.2 Effects of Strain and Strain-Induced Damage on the Electrical Resistivity of Polymer-Matrix Structural Composites

Polymer-matrix composites containing continuous carbon fibers are important for aircraft, missiles, satellites and other lightweight strategic structures. In order to enhance safety and its operation, such a structure needs to sense its condition, such as any damage to it and the strain that it is under. Damage sensing is used in structural health monitoring. Strain sensing is used in structural vibration control, stress monitoring, and weighing.

This section addresses the attainment of sensing without the need to use of embedded or attached sensors, as the structural material itself is the sensor. The ability of a structural material to sense itself is known as self-sensing. The advantages of self-sensing include low cost, high durability, large sensing volume, and an absence of mechanical properties (which tend to occur in the case of embedded sensors). Examples of embedded or attached sensors include optical fibers and piezoelectric sensors.

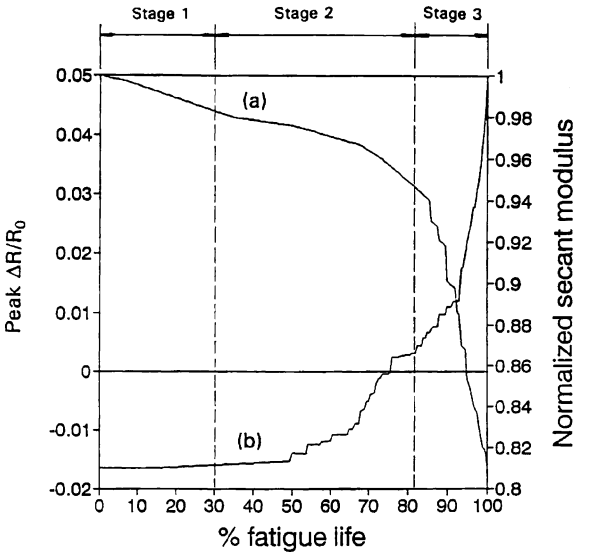

Figure 7.15. Evolution of damage in the form of fiber breakage during tension–tension fatigue, as shown by the longitudinal volume resistance. *a* Normalized secant modulus, *b* the peak value of the fractional change in resistance (relative to the initial resistance) in a stress cycle. The variation in resistance within a cycle (not shown) is due to the effect of strain rather than that of damage. (From [6])

Self-sensing is made possible by the effects of strain and damage on the electrical resistivity, which can be the volume/surface resistivity of the composite or the contact resistivity of the interlaminar interface (interface between the laminae of a continuous fiber in a composite). This ability has been shown for composites that involve carbon fibers, which are electrically conductive, in contrast to the insulating character of the polymer matrix, thereby allowing the resistivity of the composite to vary with damage or strain.

Damage in the form of fiber breakage causes the electrical conductivity in the fiber direction of the composite to decrease. In other words, the resistance increases, as shown in Fig. 7.15 for damage during tension–tension fatigue, with the stress occurring in the fiber direction of the composite. The resistance increase correlates with a decrease in the secant modulus.

Damage in the form of delamination causes the electrical conductivity in the through-thickness direction of the composite to decrease, as explained below. Although the polymer matrix is electrically nonconductive, the through-thickness conductivity of a composite is never zero due to the flow of the resin during composite fabrication and the waviness of the fiber, and the consequent direct contact between fibers that belong to adjacent laminae. The contact occurs at certain random points of the interlaminar interface. When delamination occurs, a crack occurs at this interface. This crack diminishes the extent of fiber–fiber contact, thereby causing the through-thickness conductivity of the composite to decrease. Figure 7.16 shows the increase in through-thickness resistance during tension-tension fatigue, with the stress occurring in the fiber direction of the composite.

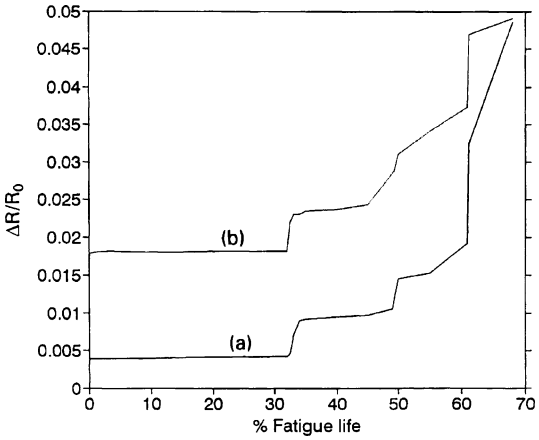

Figure 7.16. Evolution of damage in the form of delamination during tension–tension fatigue, as shown by the through-thickness volume resistance. *a* The minimum value of the fractional change in resistance (relative to the initial resistance) in a stress cycle. *b* The maximum value of the fractional change in resistance in a stress cycle. The variation in resistance within a cycle (not shown) is due to the effect of strain rather than that of damage. (From [6])

As a consequence of the effects mentioned above, the electrical conductivity (the reciprocal of the electrical resistivity) provides an indicator of the damage. By selecting the direction of conductivity measurement, different types of damage can be selectively detected.

Yet another direction of resistance measurement is the oblique direction, which is a direction between the longitudinal and through-thickness direction. The oblique resistance increases upon damage, as shown in Fig. 7.17 for the case of impact damage.

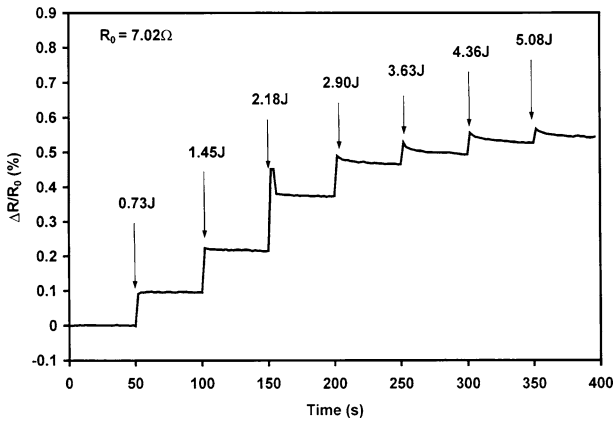

Figure 7.17. Fractional change in oblique resistance (relative to the initial resistance) vs. time during impact at progressively increasing energy. The *arrows* indicate the impact times. (From [7])

Strain sensing is particularly effective under flexure, which is one of the most common forms of loading in composite structures. Upon flexure, one side is under tension while the opposite side is under compression. The surface resistance of the side under compression decreases reversibly upon flexure due to the increase in the degree of current penetration in the through-thickness direction (Fig. 7.18a); the surface resistance of the side under tension increases reversibly upon flexure due to the decrease in the degree of current penetration in the through-thickness direction (Fig. 7.18b).

Sensing is also effective under through-thickness compression (which is relevant to fastening), as indicated by either the contact resistance of the interlaminar interface or the longitudinal resistance of the composite. Upon compression, the contact

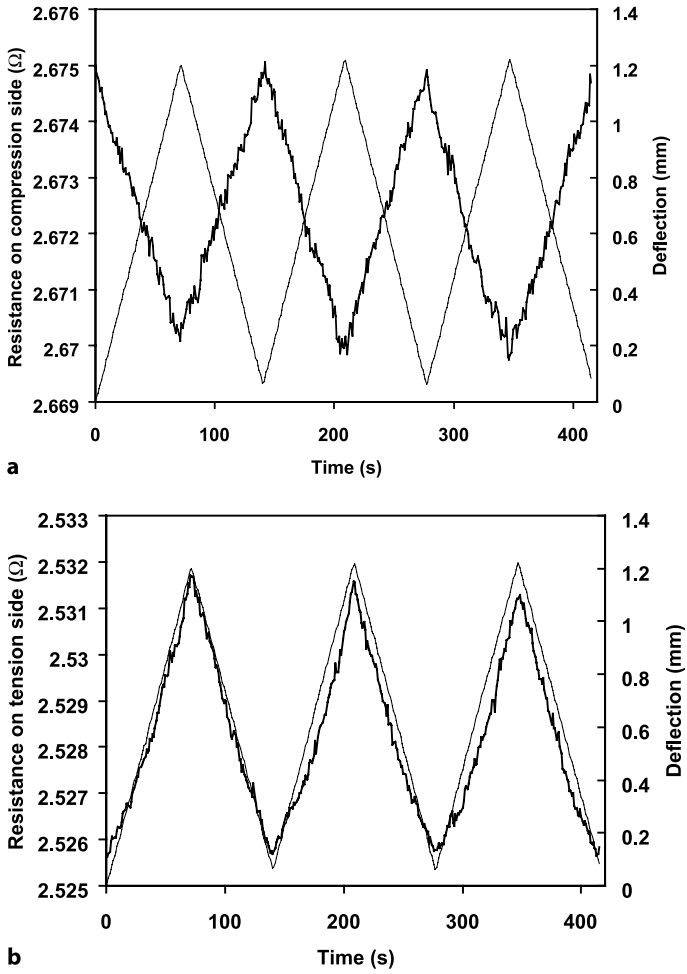

Figure 7.18. Resistance (*thick curve*) during deflection (*thin curve*) cycling at a maximum deflection of 1.199 mm (stress amplitude of 218.5 MPa). **a** Compression surface resistance, **b** tension surface resistance. (From [8])

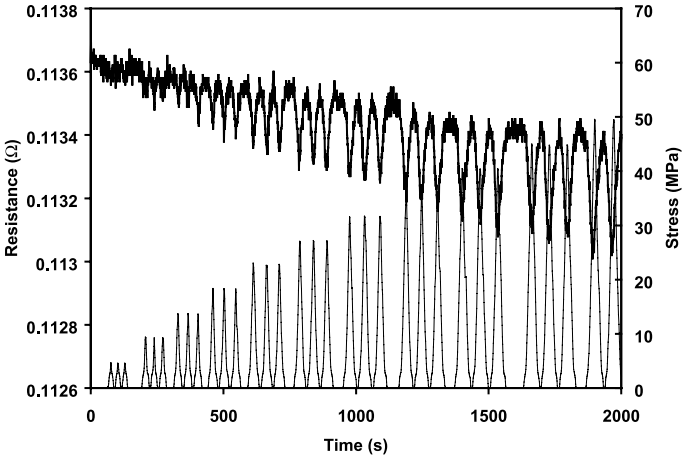

Figure 7.19. Variation in the longitudinal volume resistance (*thick curve*) with time, and of the through-thickness compressive stress (*thin curve*) with time, during through-thickness compressive stress cycling at progressively increasing stress amplitudes (three cycles for each amplitude). (From [9])

resistance of the interlaminar interface decreases (Fig. 7.19) due to increased proximity between the fibers of adjacent laminae, while the longitudinal resistance also decreases due to the decrease in through-thickness resistivity, which enables the longitudinal current to take detours around defects.

The interlaminar interface is itself a damage sensor, as the contact electrical resistivity of this interface is sensitive to minor damage, as inflicted by impact at low energy. Figure 7.20 shows the irreversible decrease in this resistivity upon

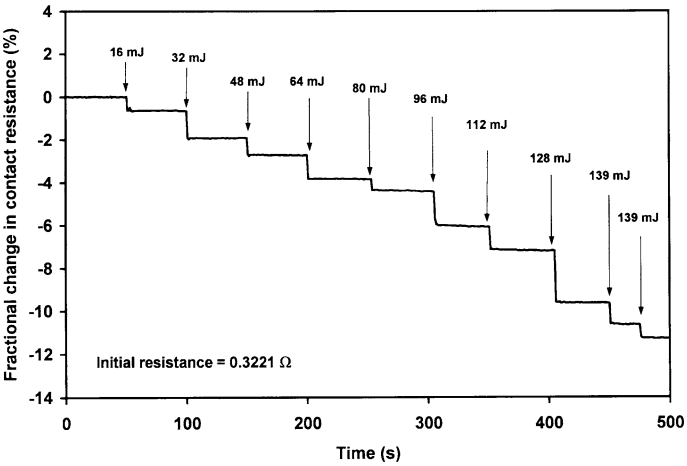

Figure 7.20. Contact resistance vs. time during impact for progressively increasing impact energies from 16 to 139 mJ, as directed onto the exterior composite surface above the interlaminar interface, which is monitored in terms of the contact electrical resistance. (From [10])

impact. The decrease in resistivity occurs at impact energies as low as 0.8 mJ. The greater the damage, the lower the resistivity. Damage causes a decrease in resistivity due to the irreversible increase in the extent of fiber–fiber contact between fibers of adjacent laminae.

In resistance measurement, the voltage and current contacts are placed along a straight line, which is the direction of resistance measurement. In contrast, in potential measurement, the voltage contacts are placed along a line that does not overlap with the line formed by the current contacts. Sensing by resistance measurement is more effective than sensing by potential measurement, although the latter is more amenable to spatially resolved sensing.

For resistance measurement, the four-probe method (with four electrical contacts, the outer two of which are for passing current and the inner two of which are for measuring the voltage) is more effective than the two-probe method (with two electrical contacts, each of which are for both current and voltage) due to the inclusion of the resistance of the electrical contacts in the resistance obtained using the two-probe method. Damage to the electrical contacts affects the two-probe resistance more than the four-probe resistance.

An analytical model is available for the piezoresistance of a continuous carbon fiber polymer-matrix composite under flexure. This phenomenon allows strain sensing and entails a reversible increase in the tension surface resistance and a reversible decrease in the compression surface resistance during flexure. The model considers that the change in surface resistance is due to the change in the degree of current penetration. The longitudinal strain resulting from the flexure affects the through-thickness resistivity (which relates to the contact resistivity of the interlaminar interface).

In summary, the self-sensing abilities of carbon fiber polymer-matrix structural composites are due to the effects of strain and damage on the electrical resistivity, which can be the volume resistivity of the composite or the contact resistivity of the interlaminar interface. Sensing is particularly effective under flexure, as indicated by the surface resistance of the side under compression or that under tension. It is also effective under through-thickness compression (which is relevant to fastening), as indicated by the longitudinal resistance of the composite. In addition, it is effective under impact, as indicated by the contact resistance of the interlaminar interface. Sensing by resistance measurement is more effective than sensing by potential measurement, although the latter is more amenable to spatially resolved sensing. For resistance measurement, the four-probe method is more effective than the two-probe method.

7.7.2.1 Effects of Strain and Strain-Induced Damage on the Electrical Resistivities of Cement-Matrix Structural Composites

Functional behavior similar to that described in Sect. 7.7.2 is exhibited by cement-matrix composites containing discontinuous and electrically conductive fibers as an admixture. Continuous fiber is not attractive due to its high cost and its unsuitability for incorporation into a cement mix.

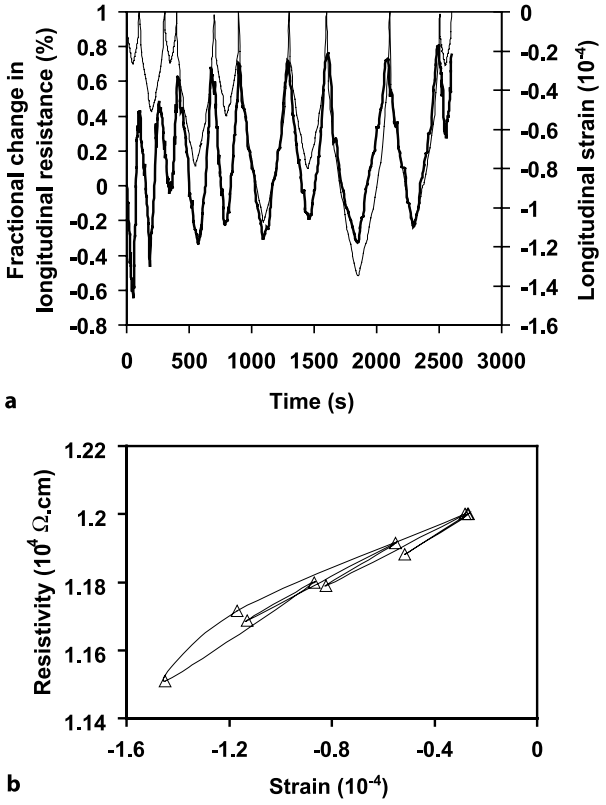

Figure 7.21. **a** Curves of fractional change in longitudinal resistance (*thick curve*) versus time and of longitudinal strain (*thin curve*) versus time using repeated compression of carbon fiber reinforced cement at various strain amplitudes. The resistance is measured using the four-probe method. **b** Variation in the resistivity at the peak strain versus the strain amplitude for the data in (**a**). The data points are connected with a *line* drawn to indicate the order in which the various strain amplitudes were imposed. The order is as shown in (**a**). (From [11])

By using carbon fiber (isotropic-pitch-based, about 5 mm long, 0.5 vol%, just below the percolation threshold, which is between 0.5 and 1.0 vol%) in cement paste (without aggregate), piezoresistivity-based strain sensing has been achieved, as shown upon repeated uniaxial compression by using the four-probe method in Fig. 7.21. The gage factor (fractional change in volume resistance per unit strain) is around 280 and the volume resistivity is around $1.2 \times 10^4\,\Omega\,\mathrm{cm}$. There is little, if any, hysteresis, as shown in Fig. 7.21b. However, when the two-probe method is used instead of the four-probe method, the strain sensing is not feasible due to poor repeatability, as shown in Fig. 7.22. In spite of the presence of piezoresistivity, with a gage factor of around 200 and a resistivity of $1.3 \times 10^4\,\Omega\,\mathrm{cm}$, the poor repeatability makes the sensing infeasible. The poor repeatability is due to the variation in the contact resistance during loading and unloading. The contact resistance is included in the measured resistance in the two-probe method.

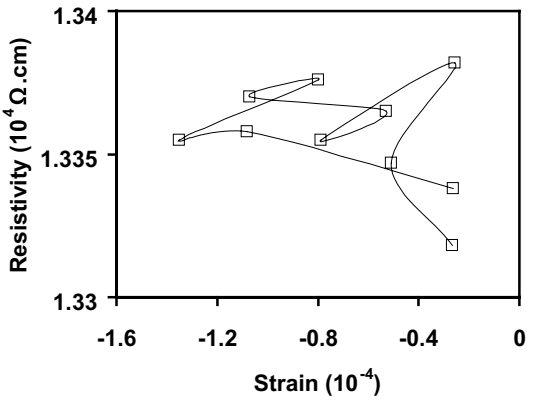

Figure 7.22. Variation in the resistivity at the peak strain versus the strain amplitude for carbon fiber reinforced cement. The resistance is measured using the two-probe method. The data points are connected with a *line* drawn to indicate the order in which the various strain amplitudes were imposed. The order is as shown in Fig. 7.21a. (From [11])

Upon flexure (three-point bending), the surface electrical resistance on the compression side decreases reversibly, while that on the tension side increases reversibly, thus allowing strain sensing (Fig. 7.23). Damage, which occurs when the deflection is sufficiently large, causes the resistance to increase irreversibly, as shown clearly for the surface resistance on the tension side. At failure, either resistance increases abruptly.

An analytical model is available to describe the piezoresistivity in carbon fiber reinforced cement (with and without embedded steel reinforcing bars) under flexure (three-point bending) [12]. The phenomenon involves the reversible increase in the tension surface electrical resistance and the reversible decrease in the compression surface electrical resistance upon flexure. The piezoresistivity is enhanced by the presence of steel rebars. The theory is based on the concept that the piezoresistivity is due to the slight pulling out of crack-bridging fibers during crack opening and the consequent increase in the contact electrical resistivity of the fiber–matrix interface.

The strain sensing ability of carbon fiber reinforced cement, as based on piezoresistivity, remains in the presence of damage. However, the gage factor is affected by strain and damage. The gage factor under uniaxial compression is diminished by compressive strain by up to 70% and is diminished by damage by up to 25%. This means that the sensing is best at low strains.

7.8 Seebeck Effect

7.8.1 Scientific Basis

When an electrical conductor is subjected to a temperature gradient, charge carriers move. The movement is typically in the direction from the hot point to the cold point of the temperature gradient, due to the higher kinetic energies of the carriers

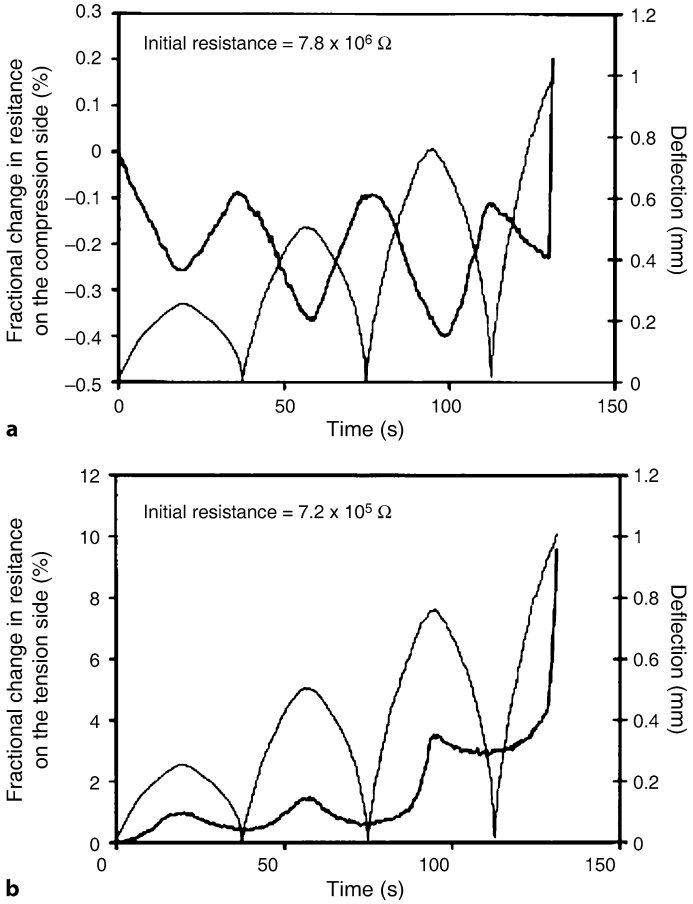

Figure 7.23. Variation in the surface resistance (*thick curve*) with time, and of the mid-span deflection (*thin curve*) with time, during three-point bending at progressively increasing deflection amplitude (up to failure) for a carbon fiber (about 5 mm long, 0.5 vol%) reinforced cement paste. **a** Resistance on the compression side, **b** resistance on the tension side. (From [13])

at the hot point. The carrier flow results in a voltage difference (called the Seebeck voltage) between the hot and cold ends of the conductor. This phenomenon is known as the Seebeck effect, which is a type of thermoelectric effect.

The Seebeck effect allows the conversion of thermal energy (associated with the temperature gradient) to electrical energy, and is the basis for thermoelectric energy generators, which are devices for generating electricity from temperature gradients. This type of electricity generation is attractive due to the absence of pollution and the fact that temperature gradients are commonplace (e.g., that between a water heater and its surroundings, that between an engine and its surroundings, etc). In other words, using the Seebeck effect, waste heat can be utilized to generate electricity.

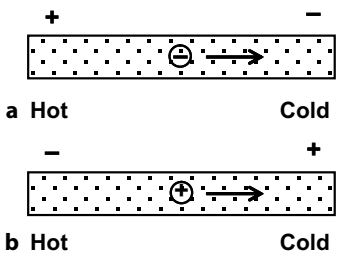

Figure 7.24. Seebeck effect due to carriers moving from a hot point to a cold point. **a** Negative carrier, **b** positive carrier

If the dominant carrier is negatively charged (as in the case of electrons), the movement results in a Seebeck voltage that has its negative end at the cold end of the specimen, as illustrated in Fig. 7.24a. If the dominant carrier is positively charged (as in the case of holes, which refer to electron vacancies), the movement results in a Seebeck voltage that has its negative end at the hot end of the specimen, as illustrated in Fig. 7.24b. It is possible for a conductor to have both electrons and holes, as in the case of a semiconductor.

The Seebeck coefficient (S; also known as the thermoelectric power or the thermopower) is defined as the negative of the Seebeck voltage divided by the temperature difference between the hot and cold ends. In other words,

$$S = -\Delta V/\Delta T \,, \tag{7.56}$$

where ΔV is the voltage difference and ΔT is the corresponding temperature difference. The units of S are V/K.

In Fig 7.24b, which shows the situation where the carrier is positive, the Seebeck coefficient is positive since ΔV and ΔT have opposite signs. In the case of Fig. 7.24a, which shows the situation where the carrier is negative, the Seebeck coefficient is negative since ΔV and ΔT have the same sign.

Carriers tend to be scattered when they collide with the thermally vibrating atoms in the solid. The extent of carrier scattering depends on the relationship of the carrier energy with the carrier momentum (i.e., the energy band structure) near the Fermi energy (the highest occupied energy level in the absence of any thermal agitation; i.e., at the temperature of 0 K). As a result of the scattering, the carriers do not necessarily move in the direction illustrated in Fig. 7.24. In other words, it is possible for a material containing negative carriers to have a positive Seebeck coefficient.

The Seebeck effect also allows the sensing of temperature, since the voltage output relates to the temperature difference. Thus, the Seebeck voltage can be used to find the temperature of one end of the conductor if the temperature of the other end is known. To measure the temperature of a hot point, it is more convenient to measure the voltage difference between two cold points rather than that between the hot point and the cold point. Therefore, two conductors that have different values of the Seebeck coefficient are used in the configuration shown in Fig. 7.25. This configuration constitutes a thermocouple, which is a device for temperature

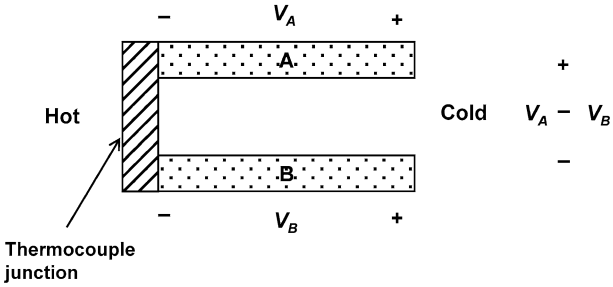

Figure 7.25. A thermocouple consisting of dissimilar conductors A and B (*dotted regions*) that are electrically connected at one end. The *shaded region* at the hot end is the conductor that electrically connects A and B

measurement. The two conductors, labeled A and B, are electrically connected at one end to form a thermocouple junction, which corresponds to the hot point (in the case where the temperature to be measured is above room temperature). The cold ends of A and B are at the same temperature (typically room temperature). The voltage difference between the hot and cold points of A is given by

$$V_{\mathrm{A}} = S_{\mathrm{A}} \Delta T \,, \tag{7.57}$$

where S_{A} is the Seebeck coefficient of A. The voltage difference between the hot and cold points of B is given by

$$V_{\mathrm{B}} = S_{\mathrm{B}} \Delta T \,, \tag{7.58}$$

where S_{B} is the Seebeck coefficient of B. The voltage difference between the cold ends of A and B is given by

$$V_{\mathrm{A}} - V_{\mathrm{B}} = (S_{\mathrm{A}} - S_{\mathrm{B}}) \Delta T \,, \tag{7.59}$$

where Eqs. 7.57 and 7.58 have been used. Equation 7.59 means that $V_{\mathrm{A}} - V_{\mathrm{B}}$ is proportional to ΔT. The greater $(S_{\mathrm{A}} - S_{\mathrm{B}})$, the more sensitive the thermocouple. Thus, A and B should be chosen to be as dissimilar as possible.

Particularly strong dissimilarity occurs when A and B contain carriers of opposite signs. In other words, S_{A} and S_{B} are opposite in sign, so that $S_{\mathrm{A}} - S_{\mathrm{B}}$ is equal to the sum of the magnitudes of S_{A} and S_{B}. Due to the resulting large voltage output, the configuration involving A and B with Seebeck coefficients of opposite sign is commonly used for thermoelectric power generation. In order to obtain an even larger voltage output, multiple junctions are used, as illustrated in Fig. 7.26, so that the A and B legs are in series and the output voltage is the sum of the voltages from all of the legs.

The Seebeck coefficient is measured using electrical leads (wires) that are made of a certain conductor (e.g., copper). The leads are attached to the hot and cold ends of the conductor under investigation, as illustrated in Fig. 7.27. The lead attached to the hot end has a temperature gradient along its length, while that attached to the cold end does not. Thus, a Seebeck voltage V_{w} occurs between the hot and cold

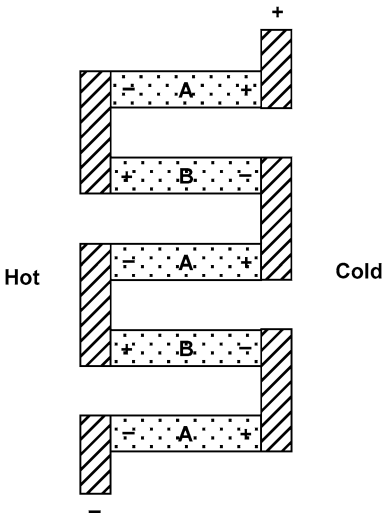

Figure 7.26. A thermoelectric energy generator consisting of a series of alternately positioned conductors A and B (*dotted regions*). The *shaded regions* are conductors that electrically connect A and B. The temperature to the left of the device is different from that to the right of the device

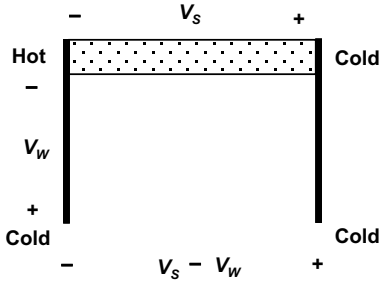

Figure 7.27. A conductor (*dotted region*) subjected to a temperature gradient, with electrical leads attached in order to measure the Seebeck voltage

ends of the wire attached to the hot end of the conductor under investigation, while a Seebeck voltage V_s occurs between the hot and cold ends of the conductor under investigation (i.e., the specimen). Thus, the measured voltage difference between the cold ends of the two leads equals $V_s - V_w$. This means that V_w must be added to this measured voltage difference in order to obtain V_s.

Based on Eq. 7.40, the electric power provided by the Seebeck effect is given by S^2/ρ, where S is the Seebeck coefficient and ρ is the electrical resistivity. Thus, S^2/ρ is known as the power factor. This means that a high value of S and a low value of ρ are preferred.

In order for a material to sustain a substantial temperature gradient, its thermal conductivity must be sufficiently low. Therefore, both a high power factor and a low thermal conductivity are necessary for a thermoelectric material used in

a thermoelectric energy generator. As a consequence, the figure of merit (Z) of a thermoelectric material is given by

$$Z = S^2/(\varrho k) \,, \tag{7.60}$$

where k is the thermal conductivity. The units of Z are K^{-1}. The dimensionless figure of merit (ZT) of a thermoelectric material is given by the product of Z and the temperature in K, where the temperature is the average temperature of the temperature gradient. A higher value of T helps to provide a higher value of ZT. Thus, a material (e.g., a ceramic material) that can withstand high temperatures is preferred. The quantity ZT relates to the thermodynamic efficiency of the energy conversion and is commonly used to describe the performance of a thermoelectric material. However, the area perpendicular to the thermoelectric direction is also important, since a larger area gives a lower resistance and hence a higher power output. Thermoelectric research has focused on raising ZT, with little attention paid to increasing the area.

The need for a low thermal conductivity and a low electrical resistivity represents a challenge. Metals do not satisfy this requirement, since they have high thermal conductivities, although their electrical resistivities are low. Electrical insulators do not satisfy this requirement, since they have high electrical resistivities. Semiconductors, on the other hand, can have reasonably low thermal conductivities and reasonably low electrical resistivities. Thus, thermoelectric materials are commonly semiconductors in the form of alloys or compounds that have been tailored for the abovementioned combination of properties. Examples are bismuth telluride (Bi_2Te_3) and lead telluride (PbTe). Another advantage of semiconductors is that they can be doped (typically through the use of a solute to form a dilute solid solution) to be n-type (i.e., a situation in which electrons are the dominant carrier) or p-type (i.e., a situation in which holes are the dominant carrier), thus providing widely dissimilar materials. However, disadvantages of the semiconductors include their high material cost and their mechanical brittleness.

A ZT value of 1 is considered to be very good. The highest ZT values reported are in the range from 2 to 3. However, a ZT value above 3 is necessary for a thermoelectric energy generator to compete with mechanical methods of electricity generation. This is why thermoelectric energy generation is currently not playing a substantial role in the energy sector. Nevertheless, due to the severity of the energy crisis, much research is being conducted to develop thermoelectric materials with higher ZT values.

As an example, a state-of-the-art Bi_2Te_3 thermoelectric thin-film material has $S = -287\,\mu V/K$ at 54°C, an electrical resistivity of $9.1 \times 10^{-6}\,\Omega\,m$, and a thermal conductivity of $1.20\,W/(m\,K)$. These values give $Z = 7.5 \times 10^{-3}\,K^{-1}$ or $ZT = 2.5$.

Due to their high thermal conductivities, metals are low in ZT. As an example of a metal, consider copper, with $S = +3.98\,\mu V/K$, electrical resistivity = $1.678 \times 10^{-8}\,\Omega\,m$ and thermal conductivity = $401\,W/(m\,K)$ at room temperature. These values correspond to $Z = 2.4 \times 10^{-6}\,K^{-1}$ or $ZT = 7.0 \times 10^{-4}$, which is tiny. Even if T is 1,000 K, ZT remains low.

A ZT value of around 2–3 is needed to provided an energy conversion efficiency of 15–20% [14]. State-of-the-art bulk thermoelectric materials have $ZT = 1.2$ at

300 K [14–16]. Thin-film thermoelectric materials can reach higher *ZT* values; e.g., 2.4 in the case of a p-type Bi_2Te_3/Sb_2Te_3 superlattice at 300 K [17]. Thin films can allow quantum confinement of the carrier, thereby obtaining an enhanced density of states near the Fermi energy. In addition, thin films can allow structures in the form of superlattices with interfaces that block phonons but transmit electrons. Due to the barrier layers needed for quantum confinement, the *ZT* value of a device with an electron gas as the active region is much higher than that of the electron gas itself [18]. For example, in the case of strontium titanate, *ZT* is 2.4 for the electron gas and 0.24 for the device [18]. Bulk thermoelectric materials are needed for practical applications. However, state-of-the-art thermoelectric materials tend to suffer from problems associated with one or more of the following: high cost of materials and processing, thermoelectric material size limitations, production scale-up difficulties, insufficiently high *ZT*, inadequate mechanical performance, and implementation difficulties.

A different thermoelectric approach involves modifying a structural material that is not thermoelectric but is widely available on a large scale. The modification gives the material thermoelectric properties. This approach results in a multifunctional structural material that can provide both structural and thermoelectric functions. Such a multifunctional material enables self-powered structures (i.e., structures that generate electric power). Self-powering is attractive for structures for which the use of batteries is not desirable, structures that power transmission lines cannot reach, and strategic structures that require back-up energy. In the case of structural materials in the form of composites with continuous fiber reinforcement, the volume fraction of the continuous fibers in the composite must be sufficiently high after the modification, since the fibers are the load-bearing component.

Imparting energy-harvesting properties to a structure through the use of a structural material that already has such properties should be distinguished from an approach that involves the use of embedded or attached devices. The latter method suffers from high cost, poor durability, mechanical property loss, and limited functional volume.

7.8.2 Thermoelectric Composites

Binary alloys such as Si-Ge and ternary alloys such as Bi-Sb-Te, all in a single-phase crystalline form, have long been investigated due to their thermoelectric behaviors. Recently, such alloys with nanoscale grain sizes have been shown to be particularly effective, since the grain boundaries inhibit heat transport but allow electron transport. Due to the combination of low thermal conductivity and high electrical conductivity, the *ZT* value is quite high. Although the term "composites" is used in the physics community for such nanostructured alloys, these materials are not composites, regardless of whether these alloys are single-phase or multiphase. This is because the structure is not formed by artificially blending the components of the structure; it is formed by high-temperature heat treatment after mixing the ingredients. The high-temperature heat treatment results in one or more phases

that are in accordance with the thermodynamics and kinetics of the material system. For example, steel is formed from its ingredients through high-temperature heat treatment and is an alloy rather than a composite. In contrast, a carbon fiber epoxy-matrix composite is indeed a composite, as it is formed by artificially blending the components. This section discusses thermoelectric composites but not thermoelectric alloys, although the development of thermoelectric composites is still in its infancy.

By sandwiching (bringing the polished surfaces into contact without bonding them) a Bi-Te compound of thickness 100 μm between 300 μm thick copper electrodes, a ZT of 8.81 at 298 K (compared to 1.04 for the Bi-Te compound itself) and a thermoelectric power of 711 μV/K (compared to 245 μV/K for the Bi-Te compound itself) were obtained in the direction perpendicular to the plane of the sandwich [19]. The ZT value in the presence of the copper electrodes decreases rapidly with increasing thickness of either the Bi-Te compound or the copper electrodes, thus leading to the conclusion that the high ZT of 8.81 is due to the large barrier thermo-emf generated in the Bi-Te region $< 50\,\mu m$ from the boundary [19]. By sandwiching (by welding) a Bi-Sb alloy of thickness 14 mm between 3 mm thick metal (either copper or nickel) electrodes, a ZT of 0.44 at 298 K (compared to 0.26 for the Bi–Sb alloy itself) and a thermoelectric power of −110 μV/K (compared to −85 μV/K for the Bi–Sb alloy itself) were obtained [20]. This means that the sandwiching [18, 19] causes significant increases in both ZT and the thermoelectric power.

A more practical example of the composite route to thermoelectric material development relates to the incorporation of a mixture of tellurium and bismuth telluride thermoelectric nanoparticles at the interface between adjacent laminae of continuous carbon fibers (fiber diameter 7 μm) in an epoxy-matrix structural composite. The use of particles that are sufficiently small is helpful, as the use of large particles would result in substantial distances between the carbon fiber laminae, thus decreasing the fiber volume fraction and hence reducing the mechanical properties. The thermoelectric particle incorporation has been shown to increase the thermoelectric power of the overall composite in the through-thickness direction (i.e., the direction perpendicular to the interlaminar interface) from 8 to 128 μV/K [21, 22]. After the thermoelectric particle incorporation, the through-thickness electrical resistivity is 0.0022 Ω cm (compared to 7.41 Ω cm for the unmodified composite; the interlaminar interface modification decreases the resistivity by three orders of magnitude) and the through-thickness thermal conductivity is 0.69 W/(m K) (compared to 0.96 W/(m K) for the unmodified composite; the thermal conductivity is decreased by the modification) [22]. Thus, for the modified composite, Z is calculated to be $0.00108\,K^{-1}$, based on Eq. 7.60, and ZT is calculated to be 0.38 at 70°C (compared to 2.8×10^{-7} for the unmodified composite) [22]. The effect of the thermoelectric particle incorporation depends on the prepreg type. In general, it is much smaller for the thermoelectric power in the longitudinal (fiber) direction of the composite [21], since the carbon fibers are the dominant influence on the longitudinal effect.

The electric power output is equal to V^2/R, where V is the voltage output and R is the resistance. The results described in the last paragraph [22] thus indicate that

the electric power output from the composite specimen (area 23 × 23 mm) is 0.46 W if the temperature difference is 70°K, and 1.3 W if the temperature difference is 120°C. Since the resistance is inversely proportional to the area, the power output is proportional to the area. In practice, the area of the composite structure can be many times larger than 23 × 23 mm, resulting in much higher power output. For example, if the area of the relevant part of a composite structure is 100 times the abovementioned area (i.e., 2.3 × 2.3 m), the power is 46 W when the temperature difference is 70°K.

A negative value for the thermoelectric power is obtained by using bismuth telluride as the main interlaminar filler. Composites that have thermoelectric power values with opposite signs can be connected in series electrically in order to obtain a large output voltage/power.

Although a polymer matrix was used in this work, alternative matrices include carbons, ceramics, and metals. These other matrices are attractive due to their abilities to withstand relatively high temperatures, hence enhancing *ZT*. A zirconia-matrix composite containing 10 vol% single-walled carbon nanotubes exhibits a *ZT* of 0.006 at 350 K and 0.017 at 850 K [23].

While thermoelectric composite engineering involving thin films is possible, it is not practical. This is because of the difficulties involved in using a thermoelectric material in the form of a thin sandwich (e.g., with a total thickness of 300 + 100 + 300 = 700 μm) [19]) in an energy conversion device.

The development of thermoelectric nonstructural composites centers on increasing *ZT* by decreasing the thermal conductivity and increasing the electrical conductivity. These composites are mainly ceramic–ceramic composites, such as B_4C-SiB_{14}-Si, B_4C-YB_6, SiB_6-TiB_2, B_4C-TiB_2, B_4C-SiC, SiB_n-SiB_4, B_4C-W_2B_5, $AgBiTe_2$-Ag_2Te, $Bi_{92.5}Sb_{7.5}$-BN-ZrO_2, $CoSb_3$-$FeSb_2$, $CoSb_3$-oxide, Ni_3B-B_2O_3 and $Ca_2CoO_{3.34}$-CoO_2. Boron carbide is particularly attractive for high-temperature thermoelectric conversion, since it has a high melting temperature. Thermoelectric nonstructural composites also include ceramic–metalloid composites, such as Bi_2Te_3-C, SiC-Si, SiB_{14}-Si and PbTe-SiGe.

Thermoelectric composites involving metals are not common, as a metal tends to increase the thermal conductivity. However, intermetallic compounds involving rare earth atoms (e.g., $CePd_3$ and $YbAl_3$) are attractive.

Thermoelectric composites are mainly designed by considering the electrical and thermal properties of the components, as a high electrical conductivity tends to be accompanied by a high thermoelectric power. For example, the addition of TiB_2 to B_4C to form the B_4C-TiB_2 composite causes *ZT* to increase due to the increase in the electrical conductivity, the slight decrease in the thermal conductivity, and the increase in the thermoelectric power. Less commonly, composites are designed by considering the interface between the components, as the interface contributes to the scattering of the carriers.

The thermal stress between a thermoelectric cell and the wall of a heat exchanger in a thermoelectric energy conversion system affects the thermal coupling as well as the durability. To reduce the thermal stress, compliant pads are used at the interface, although the pad acts as a barrier against thermal conduction. If the thermoelectric material is itself compliant, a compliant pad will not be necessary.

Metals are generally more compliant than semiconductors, but their Seebeck effects are relatively weak and they tend to suffer from corrosion. Polymers can be more compliant than metals, but they are usually electrically insulating and do not exhibit the Seebeck effect. On the other hand, a polymer containing an electrically conductive discontinuous filler (e.g., carbon black) above the percolation threshold is conductive. The use of a polymer that is an elastomer (e.g., silicone) leads to a composite that is resilient and compliant.

Electrically conductive polymer-matrix composites such as carbon black filled silicone are used for electromagnetic interference (EMI) shielding and for electrostatic discharge protection. Resilience is important when they are used as EMI gaskets. Due to the heating associated with the operation of microelectronics, which require shielding, the shielding material (particularly that associated with a mixed signal module such as one that involves both data and voice) may encounter a temperature gradient. The thermoelectric effect of the shielding material results in a voltage that may affect the performance of the microelectronics. For example, the electrical grounding may be affected. Therefore, the thermoelectric behavior of shielding materials is of concern.

An unconventional approach involves taking structural composites as a starting point and modifying these composites for the purpose of enhancing the thermoelectric properties. These structural composites are preferably ones that provide a framework that exhibits low thermal conductivity and low electrical resistivity. The modified composites are multifunctional (i.e., both structural and thermoelectric). Because structural composites are used in large volumes, imparting thermoelectric properties to these materials means that large volumes of thermoelectric materials are available for use in, say, electrical energy generation. Moreover, temperature sensing is useful for structures used in thermal control, to save energy, and in hazard mitigation. Imparting thermoelectric properties to a structural material also means that the structure can sense its own temperature without the need for embedded or attached thermometric devices, which suffer from high cost and poor durability. Embedded devices, in particular, degrade the mechanical properties of the structure.

In general, techniques for thermoelectric composite tailoring include the following. These techniques can be used in combination but they have not received adequate attention. There is much room for further research

- *Use of interfaces in a high-ZT component in the composite to decrease the thermal conductivity.* This method typically involves using the high-*ZT* component as the dominant component, so it tends to involve high material costs and to have limited design flexibility. It is commonly used to develop thermoelectric materials from semiconductors. The interfaces must hinder thermal transport but allow charge transport. In order to get a large interface area per unit volume, nanostructuring is an attractive approach.
- *Use of interfaces in a low-ZT component in the composite to decrease the thermal conductivity.* This technique does not necessarily involve a high-*ZT* component, so it tends to involve very low material costs. However, the absence of a high-*ZT*

component tends to result in a composite that does not have a particularly high *ZT*.

- *Use of a high-ZT component as the composite matrix, such that the filler is low in ZT and serves mainly to decrease the thermal conductivity and/or decrease the electrical resistivity.* This method typically involves the use of the high-*ZT* component as the dominant component in the composite, so it tends to involve high material costs and to have limited design flexibility. The *ZT* of the composite is governed by that of the high-*ZT* component.

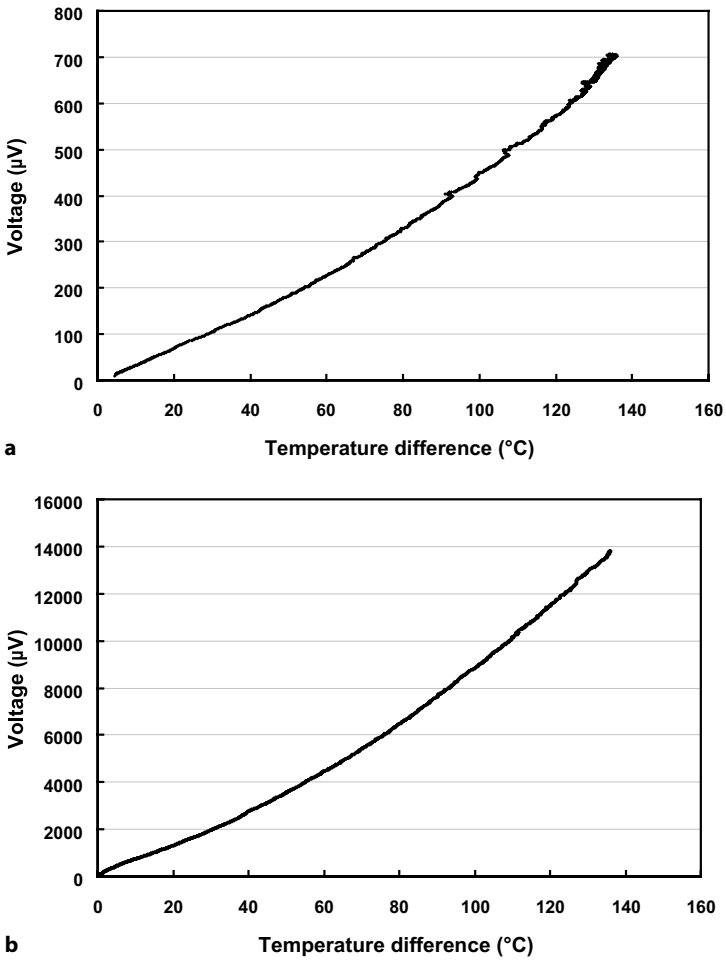

Figure 7.28. Seebeck voltage (without correction for the copper leads) vs. the temperature difference for carbon fiber epoxy-matrix composites in the through-thickness direction. **a** Without an interlaminar interface modification, **b** with tellurium and bismuth telluride particles as the interlaminar fillers, where the interlaminar interface thickness is about 33 μm. (From [22])

- *Use of a high-ZT component as a filler in the composite, such that the matrix serves to provide a framework that exhibits low thermal conductivity and low electrical resistivity.* The high-*ZT* component serves mainly to enhance the Seebeck coefficient. When the framework is a structural material, this method provides a thermoelectric structural material. It involves using the high-*ZT* component as a minor component, so it tends to have low material costs. The design of the framework is central to this technique. An example of such a framework is a continuous carbon fiber polymer-matrix composite, which exhibits a combination of low thermal conductivity and low electrical resistivity in the through-thickness direction. The waviness of the fibers causes fiber–fiber contact points between fibers of adjacent laminae across the interlaminar interface, resulting in a low through-thickness electrical resistivity, while the polymer-rich regions between the contact points at the interlaminar interface lead to a low through-thickness thermal conductivity. Fig. 7.28 shows the measured Seebeck voltage (without correction for the copper leads) vs. the temperature difference (between the hot and cold ends) for carbon fiber epoxy-matrix composites without and with tellurium (thermoelectric) particles at the interlaminar interface. The presence of tellurium and bismuth telluride nanoparticles greatly enhances the through-thickness Seebeck effect.

7.9 Applications of Conductive Materials

7.9.1 Overview of Applications

Composites for electrical conduction exhibit various levels of electrical conductivity, as needed for various applications. The highest possible level of electrical conductivity is needed for electrical interconnections in microelectronics. Less demanding levels of conductivity are needed for electrochemical electrodes, lightning protection, and electrical grounding. Still lower levels of conductivity are required for electromagnetic interference (EMI) shielding and electrostatic charge dissipation. For some applications, such as heating elements (as explained below), only an intermediate level of conductivity is required. Thus, various levels of conductivity have specific applications, and such conduction is known as controlled electrical conduction. Such materials are known as controlled resistivity materials.

By controlling the volume fraction of the conductive filler, composites with a nonconductive (or less conductive) matrix can exhibit a wide range of electrical conductivities (Fig. 7.29), as needed for various applications. Therefore, composite materials are ideally suited for use as controlled resistivity materials.

A heating element works because of the resistance (Joule or I^2R) heating that occurs when a current flows through the heating element. When the resistance is too high, there is not enough current to provide the resistance heating unless the voltage is huge. When the resistance is too low, there is not enough resistance to provide the resistance heating, even though the current is rather high. Therefore, an intermediate level of resistivity is optimum for heating elements.

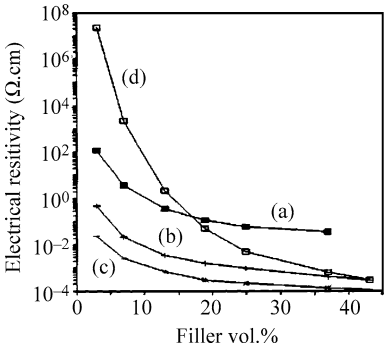

Figure 7.29. Effect of filler volume fraction on the electrical resistivity of polyethersulfone-matrix composites. *a* 0.1 μm diameter carbon nanofiber, *b* 0.4 μm diameter nickel nanofiber, *c* 2 μm diameter nickel fiber, *d* 20 μm diameter nickel fiber. (From [24])

A conductive composite commonly consists of a conductive filler in a nonconductive (or less conductive) matrix. This design is due to the fact that the matrix has the desired processability in spite of its low conductivity. For example, a polymer matrix that is nonconductive (as is the case for all conventional polymers) is attractive due to its processability (moldability) at temperatures that are not high (typically under 200°C). Processability is necessary to form articles of various shapes and sizes. Metals are highly conductive, but their processabilities are relatively low. Therefore, polymer-matrix composites are an important class of conductive materials.

For a particular conductive filler and filler volume fraction, the use of a matrix that is more conductive will result in greater electrical connectivity and hence higher conductivity for the composite. In other words, the percolation threshold is lower when the matrix is more conductive.

Polymers that are inherently conductive in the absence of conductive fillers are also available, though they are expensive and tend to be limited in terms of processability and conductivity. They utilize sp^2 hybridized carbon atoms in addition to doping (oxidation or reduction of the polymer) to increase the conductivity. Examples are polyaniline (PANI) and polypyrrole.

Carbon and cement are matrices that are conductive. Though the conductivity of cement is low, cement is attractive due to its low cost and importance in civil engineering. Depending on the heat treatment temperature, which affects the crystallinity, carbon can exhibit a wide range of conductivities.

For some applications, such as heating elements, the material needs to be able to withstand high temperatures. Polymer-matrix composites are not suitable for these applications, but carbon-matrix composites are. Unlike polymer matrices, the carbon matrix is conductive, though it is much less conductive than metals. The carbon matrix is also attractive due to its chemical resistance and low CTE. A low CTE is particularly valuable when the conductive material takes the form of a coating on a substrate (e.g., a ceramic substrate) of low CTE.

7.9.2 Microelectronic Applications

An electrical interconnection in microelectronics is a conducting line for signal transmission, supplying power, or for electrically grounding the system. It usually takes the form of a thick film of thickness > 1 μm. It can be placed on a chip, a substrate, or a printed circuit board. The thick film is created by either screen printing or plating. Thick film conducting pastes containing silver particles (the conductor) and glass frit (a binder that functions due to the viscous flow of glass upon heating) are widely used to form thick film conducting lines (interconnections) on substrates by screen printing and subsequent firing. These films suffer from a reduction in the electrical conductivity due to the presence of the glass and the porosity of the film after firing. The choice of a metal in a thick film paste depends on the need to withstand oxidation from the air during the heating process encountered upon subsequent processing, which can be the firing of the green (i.e., not sintered) thick film together with the green ceramic substrate (a process known as cofiring). It is during cofiring that bonding and sintering take place. Copper is an excellent conductor, but it oxidizes readily when heated in air. The choice of metal also depends on the temperature encountered during subsequent processing. Refractory metals, such as tungsten and molybdenum, are suitable for use in interconnections subjected to high temperatures (> 1,000°C), for example during Al_2O_3 substrate processing.

A substrate, also called a chip carrier, is a sheet on which one or more chips are attached and interconnections are drawn. In the case of a multilayer substrate, interconnections are also drawn on each layer inside the substrate, such that interconnections in different layers are connected, if desired, by electrical paths. A substrate is usually an electrical insulator. Substrate materials include ceramics (e.g., Al_2O_3, AlN, mullite, glass ceramics), polymers (e.g., polyimide), semiconductors (e.g., silicon), and metals (e.g., aluminum). The most common substrate material is Al_2O_3. As the sintering of Al_2O_3 requires temperatures of > 1,000°C, the metal interconnections need to be refractory, and thus made of materials such as tungsten or molybdenum. The disadvantage of using tungsten or molybdenum lies in their higher electrical resistivities than copper. In order to make use of more conductive metals (e.g., Cu, Au, Ag-Pd) as the interconnections, ceramics that sinter at temperatures below 1,000°C ("low temperature") can be used in place of Al_2O_3. The competition between ceramics and polymers for use as substrates is becoming fiercer. Ceramics and polymers are both electrically insulating; ceramics are advantageous in that they tend to have a higher thermal conductivity than polymers; polymers are advantageous in that they tend to have a lower dielectric constant than ceramics. A high thermal conductivity is attractive for heat dissipation; a low dielectric constant is attractive due to the reduced capacitive effect that results, reducing the signal delay. Metals are attractive due to their very high thermal conductivities compared to ceramics and polymers.

Conductive materials commonly take the form of films. There are two types of film, namely standalone films and films on substrates. Standalone films tend to be thick compared to films on substrates. Substrates are commonly electrically insulating, such as ceramics and polymers. Ceramic substrates are advantageous

compared to polymeric substrates because of their abilities to withstand high temperatures, their low CTEs, and their typically high thermal conductivities.

A *z*-axis anisotropic electrical conductor is a standalone film or an adhesive film that is electrically conducting only along the *z*-axis (in the direction perpendicular to the plane of the film). As one *z*-axis film can replace a whole array of solder joints, *z*-axis films are valuable for replacing solder, reducing processing costs, and improving repairability in surface mount technology.

Conductive films on substrates are commonly used as electrical interconnections and electrical contact pads in microelectronics. In this case, a common substrate is a printed wiring board (also called a printed circuit board), which is a polymer-matrix composite with continuous glass fiber (in the plane of the substrate), which serves to reduce the CTE. Carbon fiber is not usually used for printed wiring boards because it is conductive.

Electrically conductive joints, such as that between a wire and an electrical contact pad on a substrate, are commonly involved in microelectronics. Materials used to make such joints include solder and conductive adhesives.

7.9.3 Electrochemical Applications

Electrochemical electrodes need to be electronically conductive. In contrast, electrolytes need to be ionically conductive (i.e., ions, which can be cations and/or anions, are the charge carriers for electrical conduction). An electrochemical electrode contains an active component that participates in the electrochemical reaction. The reaction is responsible for the operation of the electrochemical device. As a result, the active component must be in contact with the electrolyte.

Since electrolytes are most commonly liquids, an electrode is commonly porous so that the electrolyte can flow into the porous electrode and thus make contact with a substantial area of the electrode. Therefore, instead of using a matrix, a small amount of binder (e.g., thermoplastic polymer particles) is used. The amount of binder used should not be excessive. There should be just enough to hold the electrode together; it should not hinder the flow of the electrolyte into the electrode. Since the electrolyte needs to make contact with the active component in the electrode, the binder should not block the active component. Therefore, the design of an electrode is quite different from that of a conventional conductor.

The active component in the electrode is not necessarily conductive, though the electrode must be conductive. For example, manganese dioxide, a common active material for cathodes, is not conductive. When the active component is not conductive, a conductive additive (e.g., carbon black) is needed to make the electrode conductive.

A current collector is an electronic conductor that is inserted into an electrochemical device (e.g., a battery) in order to allow the electric current to flow out of the device. In a common configuration, a current collector is also used as a carrier to hold the active component of the electrode. Thus, the active component of the anode releases electrons in the electrochemical reaction, and the released electrons flow to the current collector. For example, the active component takes the

form of particles that are attached to the current collector using a small amount of a binder. The amount of binder must not be excessive, as the active component and the current collector must be in electrical contact. In the less common case that the active component is a liquid, the current collector does not need to serve as a carrier; it just needs to be porous and conductive.

7.10 Conductive Phase Distribution and Connectivity

The spatial distribution of the phases can greatly affect the properties of a material. In a fibrous composite, the distribution of the fiber is important. It is particularly important when the fibers are discontinuous and present in a volume fraction below the percolation threshold. The percolation threshold is the filler volume fraction above which the filler units touch one another, forming a continuous path. When the fiber is much more conductive electrically than the matrix, percolation results in a continuous conductive path, so that the conductivity of the composite is much higher than the value below the percolation threshold.

7.10.1 Effect of the Conductive Filler Aspect Ratio

For a conductive filler in a considerably less conductive matrix, the percolation threshold decreases with increasing aspect ratio (ratio of length to width; i.e., the ratio of the length to the diameter in the case of a fiber) of the filler. This is expected from geometry, since a larger aspect ratio will make it easier for the filler units to touch one another and form a continuous path. Due to its small diameter, a nanofiber tends to have a high aspect ratio. As a consequence, a nanofiber tends to give a low percolation threshold value. A low threshold is advantageous for processability, since the processability of a composite (e.g., the ability to form it by injection molding) tends to decrease with increasing filler volume fraction. In addition, a low threshold is advantageous due to the associated cost savings and, in case of a filler of high density, weight savings too.

Although the percolation threshold tends to be low for a nanofiber compared to a microfiber, the electrical conductivity attained above percolation is relatively low for a nanofiber. This is because of the abundance of nanofiber–nanofiber contact points in a nanofiber composite and the electrical resistance associated with each contact point. Therefore, nanofibers are typically not effective at providing composites of high electrical conductivity. For example, among nickel fibers with diameters of 20 and 2 μm and nickel nanofibers with diameters of 0.4 μm, all used in the same thermoplastic polymer matrix, the nickel fibers of diameter 2 μm gave composites with the highest conductivity, whether the percolation threshold was exceeded or not (Fig. 7.29). In this context, a "nanofiber" has a diameter of less than 1 μm, whereas a "fiber" has a diameter of more than 1 μm. In Fig. 7.29, the electrical resistivity decreases with increasing filler volume fraction for each type of filler. For all other fillers than the 20 μm diameter nickel fibers, the resistivity levels off as the filler concentration increases. However, for the 20 μm diameter

nickel fiber, the resistivity does not level off, even at the highest filler volume fraction of 43%. Not leveling off means not achieving percolation. In other words, percolation is relatively difficult for the 20 μm diameter nickel fiber. Thus, there is an optimum diameter for reaching a low resistivity. This is because a diameter that is too large means that percolation becomes difficult, whereas a diameter that is too small causes a large density of high-resistance contact points between adjacent filler units.

7.10.2 Effect of the Nonconductive Thermoplastic Particle Viscosity

Figure 7.30 shows the abrupt drop in resistivity by orders of magnitude at the percolation threshold in the case of nickel particles (1–5 μm) in a thermoplastic matrix that is made from thermoplastic particles by compression molding above T_g. Two kinds of thermoplastics are used, namely polyethersulfone (PES) of particle size 100–150 μm and T_g = 220–222°C, and polyimidesiloxane (PISO) of particle size 50–100 μm and T_g = 220°C. The percolation threshold is 5 vol% for the PISO-matrix composite. For PES, the drop in resistivity is not as sharp and occurs over 4–10 vol% Ni.

When the composite is fabricated from a mixture of a conductive filler and a nonconductive matrix that takes the form of thermoplastic particles, the viscosity of the thermoplastic particles above T_g and the size of the thermoplastic particles relative to that of the filler affect the conductivity of the resulting composite. When the thermoplastic particles are considerably larger than the filler particles, small filler particles surround each thermoplastic particle in the mixture, as illustrated in Fig. 7.31a. This means that the presence of the thermoplastic particles results in the segregation of the filler particles, thereby promoting percolation. During subsequent fabrication of the composite under heat and pressure, the thermoplastic particles deform. The viscosity of a thermoplastic decreases with increasing

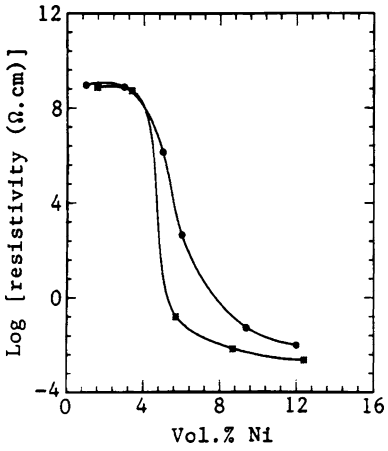

Figure 7.30. Effect of nickel particle volume fraction on the electrical resistivity of nickel particle thermoplastic-matrix composites. *Upper curve*: PES-matrix composites, *lower curve*: PISO-matrix composites. (From [25])

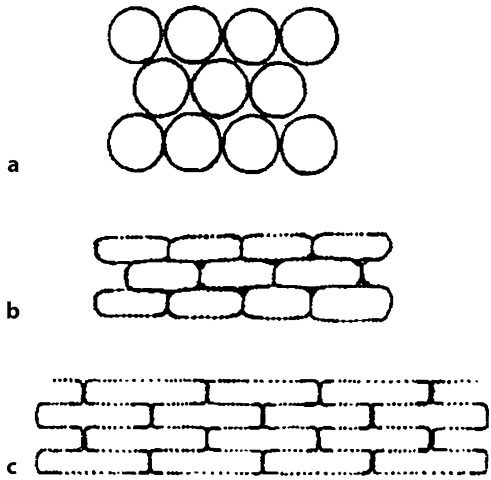

Figure 7.31. Segregation of conductive filler particles on the surfaces of larger thermoplastic particles. **a** Before compression molding, **b** after compression molding for a thermoplastic with a high viscosity, **c** after compression molding for a thermoplastic with a low viscosity. (From [25])

temperature. The lower the viscosity of the thermoplastic at the processing temperature above T_g, the greater the deformation at a given pressure, the greater the separations of some of the adjacent conductive particles, and hence the higher the resistivity of the composite after cooling to room temperature. In other words, the flow of the thermoplastic at the fabrication temperature of the composite tends to

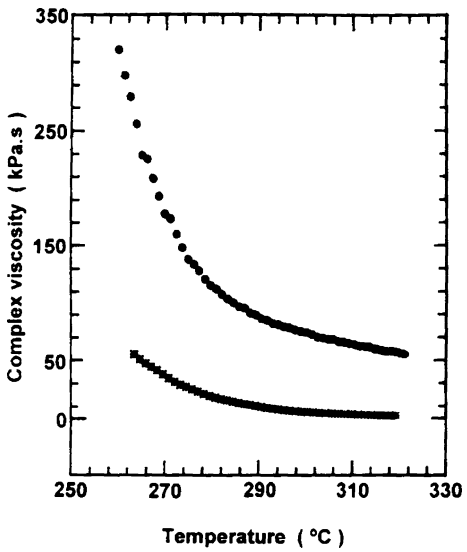

Figure 7.32. Effect of temperature on the viscosity of a thermoplastic polymer in the absence of a filler, *lower curve*: PES, *upper curve*: PISO. (From [25])

disturb the connectivity of the conductive filler particles achieved prior to heating. Figure 7.31b illustrates the structure of a composite with a high-viscosity thermoplastic, whereas Fig. 7.31c illustrates the structure of a composite with a low-viscosity thermoplastic.

At the same temperature, the viscosity is higher for PISO than PES, as shown in Fig. 7.32. As a consequence, the resistivity is lower for the PISO-matrix composite than the PES-matrix composite, as shown in Fig. 7.30.

7.10.3 Effect of Conductive Particle Size

The ratio of the size of the thermoplastic particles used to make the matrix to that of the conductive particles affects the resistivity of the composite. The higher the ratio, the lower the resistivity. This is due to the segregation of the conductive particles, as illustrated in Fig. 7.31a. A greater local concentration of the conductive particles occurs when the ratio is higher. Figure 7.33 shows the resistivities of polyimidesiloxane (PISO) matrix composites made from PISO particles of size 50–100 μm using conductive particles of various sizes. The resistivity is relatively low for composites with silver particles (0.8–1.35 μm) or nickel particles (1–5 μm) due to the high values (30 or more) of this ratio. However, it is relatively high for composites with nickel particles (78–127 μm) or graphite flakes (25 μm) due to the low values (much below 30) of this ratio. The graphite flakes give a relatively low resistivity due to their large aspect ratio.

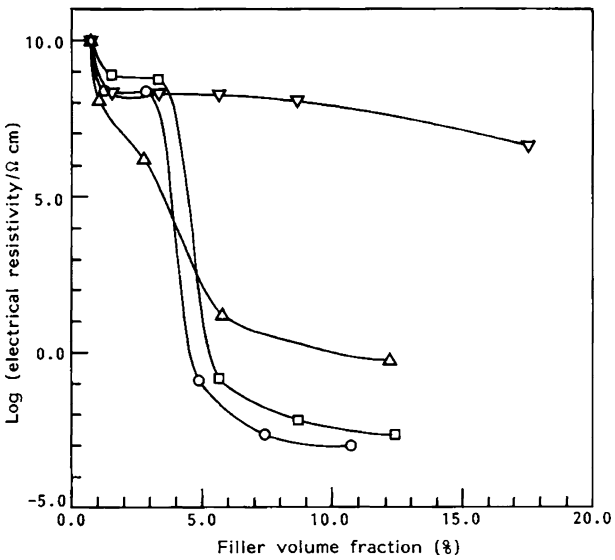

Figure 7.33. Effect of the conductive particle volume fraction on the electrical conductivities (log scale) of polyimidesiloxane-matrix composites. *Circles* – silver (0.8–1.35 μm); *squares* – nickel (1–5 μm); *inverted triangles* – nickel (78–127 μm); *triangles* – graphite flakes (25 μm). The polyimidesiloxane particle size was 50–100 μm. (From [26])

7.10.4 Effect of Additives

The additives present in a composite can affect the phase distribution, as illustrated below for the distribution of short fibers in cement. The distribution of short fibers in cement is greatly affected by the admixture (the additives present in the cement mix). Due to the high electrical conductivity of carbon fiber compared to cement, the electrical conductivity of carbon fiber reinforced cement reflects the degree of fiber dispersion. At a given fiber volume fraction, the conductivity increases with increasing degree of fiber dispersion. The lower the degree of fiber dispersion, the more severe the fiber clumping (Fig. 2.10) and, as a consequence, the less effective the fibers are at increasing the conductivity of the cement.

Figure 7.34 shows the effects of the fiber volume fraction and the admixture on the conductivity ratio, which is defined as the ratio of the measured conductivity to a calculated idealized conductivity. For the sake of simplicity, the calculated idealized conductivity is obtained using the rule of mixtures (ROM), with the fibers taken to be continuous and unidirectional in the direction of conductivity measurement and the matrix conductivity taken to be the measured conductivity of the matrix with the corresponding admixture(s) in the absence of fiber. ROM refers to weighted averaging using the volume fraction of the components as weights in

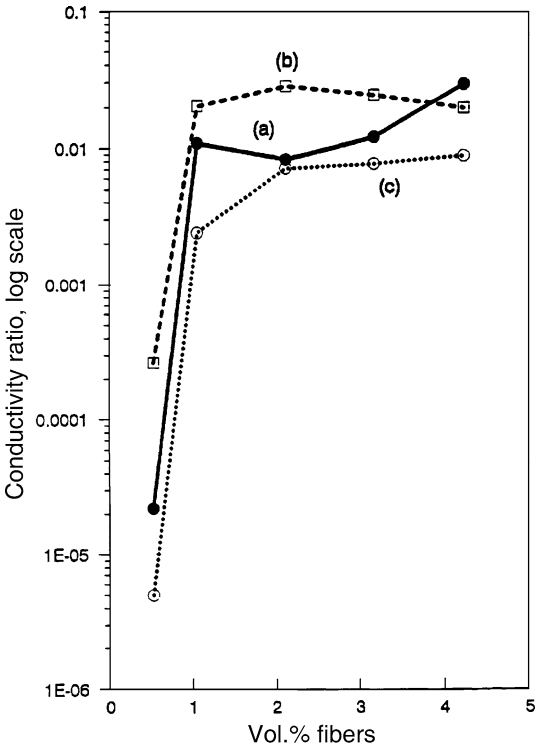

Figure 7.34. Effect of carbon fiber volume fraction on the conductivity ratio of carbon fiber cement paste. *a* With methylcellulose, *b* with methylcellulose and silica fume, *c* with latex (20% by mass of cement) . (From [27])

the averaging. In other words,

$$\begin{aligned}&\text{Calculated idealized conductivity}\\&= (\text{conductivity of fiber}) \times (\text{volume fraction of fiber})\\&= +(\text{conductivity of matrix}) \times (\text{volume fraction of matrix}) ,\end{aligned} \tag{7.61}$$

where

$$(\text{volume fraction of fiber}) + (\text{volume fraction of matrix}) = 1 . \tag{7.62}$$

The greater the conductivity ratio, the higher the degree of fiber dispersion. Microscopic examinations are not capable of discerning small differences in the degree of fiber dispersion. In contrast, the conductivity ratio approach is highly sensitive to small differences in the degree of fiber dispersion, as illustrated below.

Figure 7.34 shows that, for the same fiber volume fraction, the conductivity ratio is highest for methylcellulose with silica fume, lower for methylcellulose, and lowest for latex. Figure 7.35 shows that, for a fixed fiber volume fraction, the conductivity ratio decreases with increasing latex content. This means that the combined use of methylcellulose and silica fume gives the highest degree of fiber dispersion, whereas the use of latex gives the lowest degree of fiber dispersion, and that the degree of fiber dispersion decreases with increasing latex content. Figure 7.34 also shows that the percolation threshold is between 0.5 and 1.0 vol% carbon fiber, whichever admixture is used.

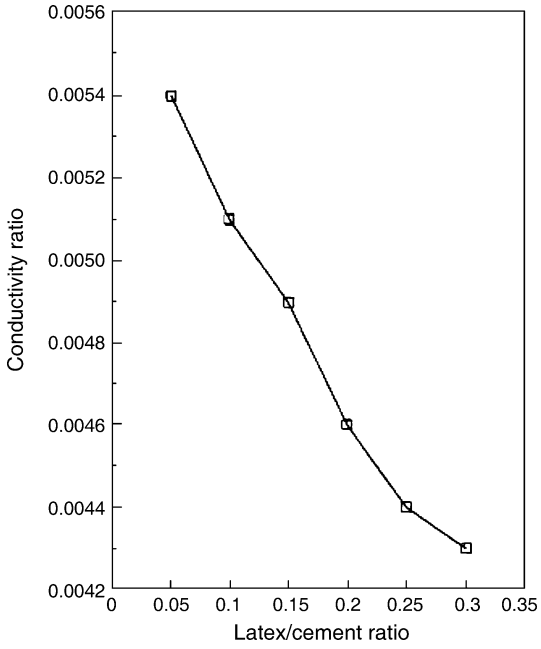

Figure 7.35. Effect of latex/cement ratio (by mass) on the conductivity ratio of carbon fiber (0.53 vol%) cement paste (from [27])

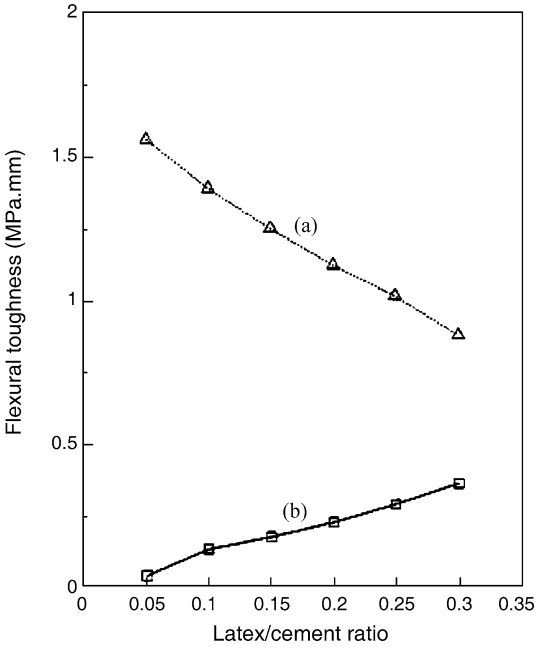

Figure 7.36. Effect of latex/cement ratio (by mass) on the flexural toughness of cement paste. *a* With carbon fiber (0.53 vol%), *b* without fiber. (From [27])

For a given fiber volume fraction, the higher the degree of fiber dispersion, the greater the flexural toughness, which is the area under the curve of flexural stress vs. midspan deflection up to failure. This is because fiber pull-out during deformation provides a mechanism for energy dissipation, and toughness is a measure of the amount of energy absorbed prior to failure. As shown in Fig. 7.36, for a fixed fiber volume fraction (0.53%), the flexural toughness decreases monotonically with increasing latex content. This is because of the decrease in the degree of fiber dispersion with increasing latex content (Fig. 7.35). On the other hand, in the absence of fiber, the flexural toughness increases monotonically with increasing latex content (Fig. 7.35) due to the viscoelastic mechanism of damping provided by latex.

At a fixed carbon fiber volume fraction of 0.53%, the flexural strength increases with increasing latex/cement ratio up to 0.15 and decreases upon increasing the latex/cement ratio further, as shown in Fig. 7.37. This is because of the effect of the latex/cement ratio on the air void content (Fig. 6.18). The air void content is lowest at the intermediate latex/cement ratio of 0.15, thus causing the flexural strength to be greatest at this latex/cement ratio. The flexural strength is sensitive to voids since voids tend to facilitate failure and the strength reflects the stress needed to cause failure. On the other hand, in the absence of fiber, the flexural strength increases monotonically with increasing latex/cement ratio (Fig. 7.37) due to the monotonic decrease in the air void content with increasing latex/cement ratio (Fig. 6.18).

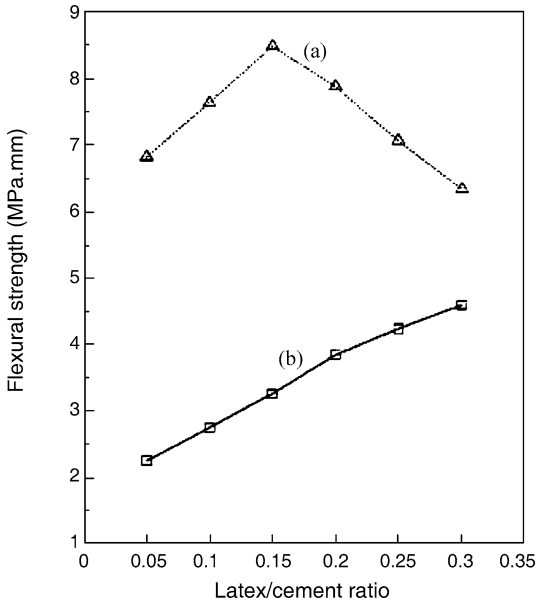

Figure 7.37. Effect of the latex/cement ratio (by mass) on the flexural strength of cement paste. *a* With carbon fiber (0.53 vol%), *b* no fiber. (From [27])

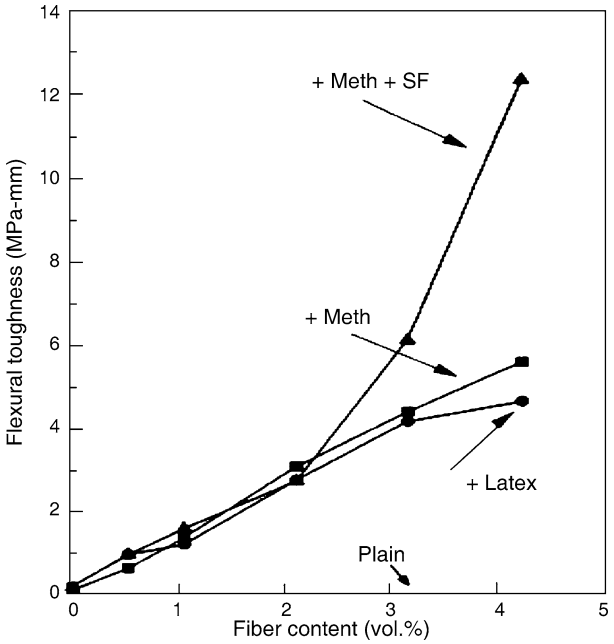

Figure 7.38. Effect of carbon fiber volume fraction on the flexural toughness of cement paste. Meth – methylcellulose (0.4% by mass of cement). SF – silica fume (15% by mass of cement). Latex – aqueous latex particle dispersion (20% by mass of cement). (From [27])

Figure 7.38 shows that, for a given fiber volume fraction, the flexural toughness is highest for methylcellulose with silica fume and lowest for latex. This is consistent with Fig. 7.34, which shows that methylcellulose with silica fume gives the highest degree of fiber dispersion, while latex gives the lowest degree of fiber dispersion. As mentioned above, the toughness is sensitive to the degree of fiber dispersion due to the mechanism of fiber pull-out for energy dissipation.

7.10.5 Levels of Percolation

In a cement-matrix composite containing a fine aggregate (typically sand) – a composite known as mortar – the cement paste (including fibers or other admixtures that may be present) can be considered to be the matrix, while the aggregate is the filler. The connectivity of the matrix is important if the matrix is conductive (as is the case when carbon fiber is present) and mortar conductivity is desired. When the conductive fibers in the cement matrix percolate (i.e., become connected due to the fiber volume fraction exceeding the percolation threshold) and the cement matrix in the mortar also percolates (since the fine aggregate volume fraction is sufficiently high), high mortar conductivity is possible and double percolation is said to occur. However, when conductivity is not needed, connectivity of the cement matrix in the mortar is usually not desirable, because the continuity promotes liquid permeability.

In a cement-matrix composite containing a fine aggregate (typically sand) and a coarse aggregate (typically gravel) – a composite known as concrete – the mortar can be considered the matrix, while the coarse aggregate is the filler. The conductivity of the mortar is important if the mortar is conductive and conductivity in the concrete is desired. When the conductive fibers in the cement matrix percolate (due to the fiber volume fraction being sufficiently high), the cement matrix in the mortar percolates (due to the fine aggregate volume fraction being sufficiently high), and the mortar in the concrete also percolates (due to the coarse aggregate volume fraction being sufficiently high), high concrete conductivity is possible and triple percolation is said to occur.

Various levels of percolation can also occur in polymer-matrix composites. For example, double percolation can occur when the composite is created from two kinds of pellets, one of which is nonconductive (due to the absence of a conductive filler), while the other is conductive (due to the presence of a conductive filler beyond the percolation threshold). If the conductive pellets form a continuous path in the composite, double percolation occurs. In this case, double percolation is advantageous since it reduces the amount of conductive raw material needed.

7.11 Electrically Conductive Joints

Electrically conductive joints, also known as electrical connections, are needed in electronics. They are mechanical joints with low electrical resistance. An electrical connection must have a resistance that is below a certain value in order for it

to be acceptable. The electrical resistance is sensitive to minor changes in the microstructure, such as the microstructure of the joint interface. Even when the mechanical aspects of the joint are acceptable, its electrical performance may not be. Electrical failure and mechanical failure may not occur simultaneously. A drop in stress due to mechanical debonding is not necessarily accompanied by an increase in the electrical resistance, particularly when the joining medium is ductile (e.g., in the case of solder). When the joining medium is relatively brittle, as in a silver-epoxy conductive adhesive, there is a greater tendency for an abrupt increase in resistance to accompany mechanical debonding. Due to the large number of electrical connections in a microelectronic package, the reliability of the connections is of great importance.

7.11.1 Mechanically Strong Joints for Electrical Conduction

With the exception of joints obtained by thermoplastic welding, soldered, brazed and welded joints are all conductive. Among these, soldered joints involve the lowest processing temperatures, so they are the joints most commonly used in electronics, since circuitry can be harmed by elevated temperature processing.

Soldering is commonly conducted by applying a flux that removes metal oxides, thereby promoting the wetting of the working metal surface by the molten solder during soldering. An example of a flux is aluminum chloride (rosin) for soldering tin.

In order to increase the density of an electronic package, a two-dimensional array of soldered joints between the contact pads on two surfaces is needed. Most commonly, one surface is the chip (i.e., the semiconductor device), while the other surface is the substrate. The chip is flipped, so that its contact pads are facing the top surface of the substrate, with the contact pads of the chip aligned with those on the substrate, as illustrated in Fig. 7.39. Each soldered joint in the array (known as a ball grid array) contains a solder sphere (called a solder bump or a solder ball), which can be applied by evaporation, electroplating, printing, direct placement, or other methods. The joints are formed by heating each solder bump to melt it, such that the molten solder remains on each contact pad. After joint formation, a nonconductive adhesive such as an epoxy is used to fill the region between the bumps in order to improve the thermal fatigue resistance of the joint. The thermal fatigue stems from the CTE mismatch between the chip and the substrate. The adhesive is known as an underfill.

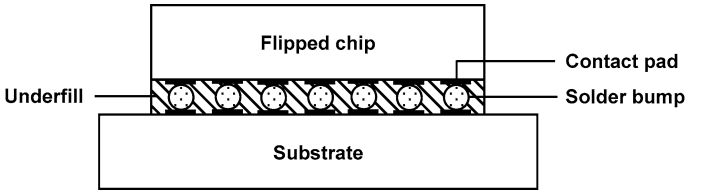

Figure 7.39. Flip chip electronic assembly involving an array of solder bumps

Solder used for printing (such as screen printing to form a two-dimensional pattern) is applied in the form of a paste called a solder paste. The paste is a slurry of solder particles in a vehicle that is a flux as well as an adhesive that provides temporary joining prior to soldering. During subsequent soldering (known as reflow soldering), every solder particle in the paste melts.

There are numerous problems with soldered joints. One problem stems from the usual presence of lead in the solder. The most common solders are tin-lead alloys near the eutectic composition. Lead is poisonous, though it aids the rheology of the solder. Therefore, lead-free solders (e.g., SnAgCu alloys) are rapidly gaining in importance, although the higher processing temperature required for them causes complications during the associated manufacturing processes.

Soldered joints also suffer from their tendency to degrade due to thermal fatigue and creep. Thermal fatigue is associated with temperature variations between the on and off states of the electronics, and stems from the difference between the thermal expansion coefficients of the two members joined by the solder.

Creep arises due to the viscoelastic behavior of solder in the solid state. Due to the low melting temperature of solder, this creep is substantial when the electronics is at its operating temperature. The creep resistance of solder can be increased by incorporating nanoparticles into the solder (i.e., by forming a particulate metal-matrix composite). The particles also serve as reinforcement besides restraining the solder from creep. The particles are nanosized in order to reduce the tendency for the particles to become nonuniformly distributed (due to the difference in density between the metal and the particles) when the solder is molten. In order for the molten solder to remain sufficiently fluid, the volume fraction of the particles must be low.

Another method of increasing the creep resistance is to use a metal-matrix composite with a solder alloy as the matrix and a continuous fiber as the reinforcement. The composite takes the form of a sheet (called a solder preform), with the fiber in the plane of the sheet. The solder preform is also attractive because of its low CTE, which is due to the low CTE of the fiber. However, the application of solder preforms is limited to planar joints.

A further issue is the reaction between the solder and a member (e.g., copper) and the formation of intermetallic compounds at the joint interface. The intermetallic compounds hinder the wetting of the member by the molten solder.

Furthermore, solder produces a large footprint on the circuit board to which the solder is applied. This large footprint is a consequence of the high fluidity of the molten solder, and is undesirable for the miniaturization of microelectronics, as it makes the fine-pitch patterning of interconnection lines difficult.

Yet another complication with soldering is the need to use flux, which is necessary to reduce the copper oxide on the copper to which the solder is bonded. Although tin-lead solder attaches well to copper, it does not attach well to copper oxide, which forms readily on copper at the soldering temperature. Flux also acts as a wetting agent during soldering; in other words, it reduces the surface tension of the molten solder so that the molten solder can wet the surfaces of the members to be joined. Due to the chemical reactivity of the flux, the flux needs to be

removed after soldering. Some fluxes require volatile organic compounds (VOCs, which contribute to air pollution) for their removal.

Due to the numerous problems associated with soldering, the replacement of soldered joints by conductive adhesive joints is being actively pursued. Conductive adhesives are polymeric adhesives (e.g., epoxy resin) that contain conductive fillers (e.g., silver particles). The conductive filler units (e.g., the silver particles) must touch one another in order to form a continuous conductive path. To achieve this, the conductive filler volume fraction needs to exceed the percolation threshold. Even when the percolation threshold is exceeded, the electrical conductivity is considerably below that of a metal, due to the contact resistance at the interface between contacting filler units. Therefore, the use of fillers that melt during the processing (the melting enables the bonding of the filler units with one another) is a method that is being investigated to achieve electrical conductivity that approaches that of a metal.

The most common conductive epoxy on the market is silver epoxy, which contains a high proportion of silver particles in an epoxy resin. For example, the silver epoxy Circuitworks CW2400 of Chemtronics contains 60–90 wt.% silver, 10–25 wt.% epoxy resin, and 1–3 wt.% modified epoxy ester. An epoxy ester is epoxy resin that has been partially esterified with fatty acids, which react with both the epoxide and the hydroxyl groups of the epoxy resin to form the ester. The epoxy ester enhances the chemical resistance. This product comes in two parts, one of them being the epoxy and the other the hardener. Curing conducted at room temperature takes 8 h, though it can be hastened by heating. The volume electrical resistivity of the product after curing is 0.001 Ω cm, which is higher than that of solders by orders of magnitude. For example, the electrical resistivity of the eutectic tin-lead solder is $1.4 \times 10^{-5}\,\Omega\,\mathrm{cm}$.

The electrical resistance of an electrical connection is the sum of the volume resistance within the joining medium (e.g., solder) and the resistance of the interface between the joining medium and each of the two surfaces to be joined. The volume resistance R_v of the joining medium is governed by the volume resistivity ϱ_v of the medium:

$$R_\mathrm{v} = \varrho_\mathrm{v} l/A \,, \tag{7.63}$$

where A is the geometric area of the electrical connection and l is the length of the joining medium in the direction perpendicular to the joint area.

The interfacial resistance R_i is governed by the interfacial resistivity ϱ_i, which depends on the microstructure of the interface, i.e.,

$$R_\mathrm{i} = \varrho_\mathrm{i}/A \,. \tag{7.64}$$

The overall resistance R of the connection is given by

$$R = R_\mathrm{v} + 2R_\mathrm{i} \,. \tag{7.65}$$

The contact resistivity of the electrical connection is given by

$$\varrho = RA \,. \tag{7.66}$$

In the case of an eutectic tin-lead electrical connection between copper surfaces, with $A = 4.2 \times 3.0\,\text{mm}^2$ and $l = 125 \pm 75\,\mu\text{m}$, the contact resistivity $\rho = 2.5 \times 10^{-4}\,\Omega\,\text{cm}$ [28]. Using Eq. 7.66,

$$R = \rho/A = 2.0 \times 10^{-3}\,\Omega\,. \tag{7.67}$$

Using Eq. 7.63, with $\rho_v = 1.4 \times 10^{-5}\,\Omega\,\text{cm}$ and $l = 125\,\mu\text{m}$,

$$R_v = \rho_v l/A = 1.4 \times 10^{-6}\,\Omega\,, \tag{7.68}$$

which is negligible compared to R. Hence, using Eq. 7.65,

$$R_i = (R - R_v)/2 \approx R/2 = 1.0 \times 10^{-3}\,\Omega\,, \tag{7.69}$$

And, using Eq. 7.64,

$$\rho_i = R_i A = 1.3 \times 10^{-4}\,\Omega\,\text{cm}\,. \tag{7.70}$$

In case of a CW 2400 silver epoxy electrical connection between copper surfaces, with $A = 5.1 \times 4.9\,\text{mm}^2$ and $l = 152 \pm 76\,\mu\text{m}$, the contact resistivity $\rho = 6.7 \times 10^{-4}\,\Omega\,\text{cm}$ [28]. Thus,

$$R = \rho/A = 2.7 \times 10^{-3}\,\Omega\,. \tag{7.71}$$

With $\rho_v = 1 \times 10^{-3}\,\Omega\,\text{cm}$ and $l = 152\,\mu\text{m}$,

$$R_v = \rho_v l/A = 6.1 \times 10^{-5}\,\Omega\,, \tag{7.72}$$

which is negligible compared to R. Hence,

$$R_i = (R - R_v)/2 \approx R/2 = 1.4 \times 10^{-3}\,\Omega\,, \tag{7.73}$$

and

$$\rho_i = R_i A = 3.4 \times 10^{-4}\,\Omega\,\text{cm}\,. \tag{7.74}$$

In spite of the much higher ρ_v of silver epoxy compared to solder, ρ and ρ_i are comparable for these two types of electrical connections. This means that ρ_i rather than ρ_v governs the electrical resistance of the overall connection. Therefore, studying the interface between the joining medium and each of the two surfaces to be joined is critical to understanding the science of the overall connection. However, research in this area has focused on ρ_v, with relatively little attention paid to ρ_i.

Figure 7.40 shows that the contact electrical resistivity of an eutectic tin-lead (63 wt.% tin, 37 wt.% lead) soldered joint (i.e., the resistance of the joint multiplied by the geometric area of the joint) between copper surfaces increases reversibly by 15% upon compression of the joint (with a stress of only 0.12 MPa) in the direction perpendicular to the joint interface. Mechanical deformation due to the compression would have caused dimensional changes that increased the resistance. Thus,

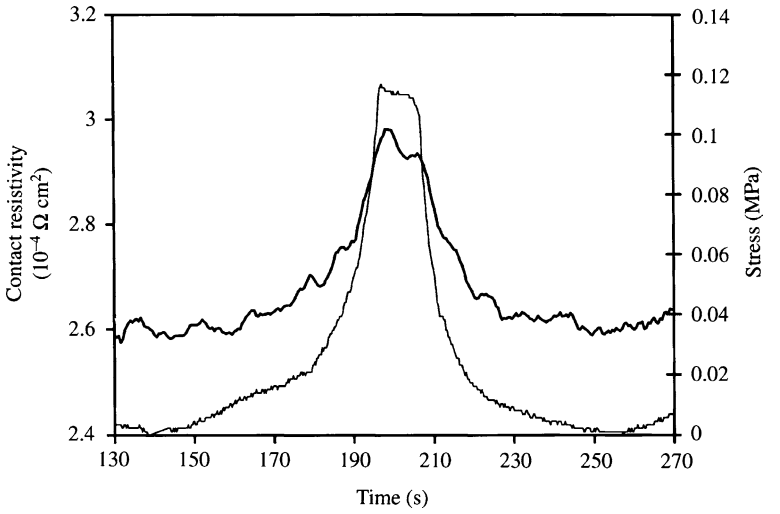

Figure 7.40. Soldered joint as an electrical connection between copper surfaces. The contact electrical resistivity of the joint increases reversibly upon compression of the joint in the direction perpendicular to the joint interface, due to a subtle reversible microstructural change at the solder–copper interface. *Thick curve*: resistivity, *thin curve*: stress. (From [28])

the observed resistance increase cannot be due to the mechanical deformation of the solder. After all, the volume resistance of the solder barely contributes to the overall resistance of the connection. The observed resistance increase is believed to be due to a subtle reversible microstructural change at the solder–copper interface. This microstructural change has not yet been identified, but it may be related to a decrease in the true contact area at the solder–copper interface (i.e., a decrease in the number of contact points across the interface) upon compression. This true contact area decrease may be related to the effect of compression on the brittle intermetallic compound (formed during soldering due to the reaction between the molten solder and the copper) at the interface.

Figure 7.41 shows that the contact electrical resistivity of a silver epoxy (room temperature cured, without postcuring) joint between copper surfaces increases reversibly by 4.5% upon compression of the joint (with a stress of only 0.04 MPa) in the direction perpendicular to the joint interface. The observed resistance increase cannot be due to the mechanical deformation of the silver epoxy. It is believed to be due to a subtle reversible microstructural change at the adhesive–copper interface.

Figure 7.42 shows that the contact resistivity ϱ of the soldered joint mentioned above increases quite reversibly by up to 6% with increasing temperature up to 50°C. For the adhesive joint mentioned above, the contact resistivity increases by up to 48% with increasing temperature up to 50°C. Thus, the thermal reliability of the soldered joint is superior to that of the adhesive joint.

The abovementioned experimental results show that the performance of an electrical connection depends on both temperature and pressure. Figure 7.43 shows the combined effects of temperature and compression on the contact electrical resistivity ϱ for an adhesive joint (silver epoxy without postcuring, between cop-

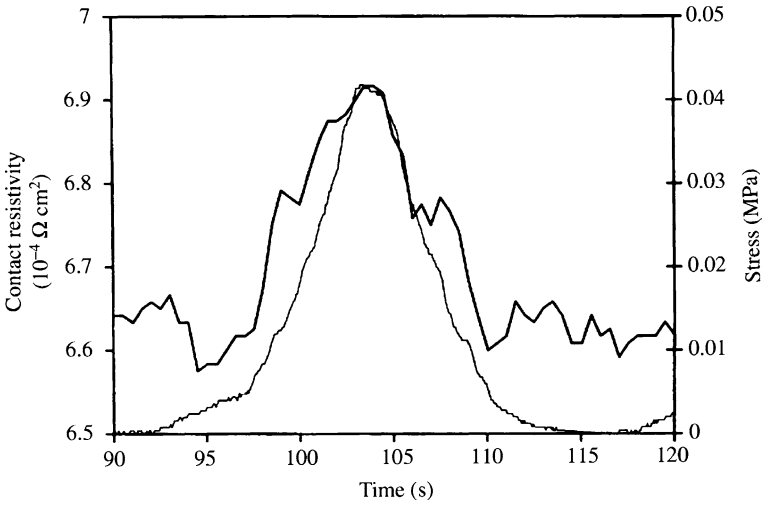

Figure 7.41. Conductive adhesive (silver epoxy without postcuring) joint as an electrical connection between copper surfaces. The contact electrical resistivity of the joint increases reversibly upon compression of the joint in the direction perpendicular to the joint interface, due to a subtle reversible microstructural change at the adhesive–copper interface. *Thick curve*: resistivity, *thin curve*: stress. (From [28])

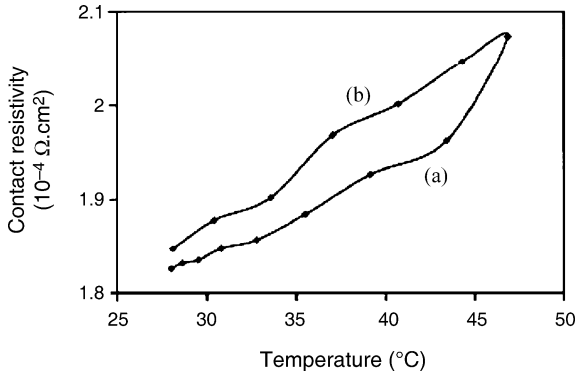

Figure 7.42. Variation in the contact resistivity ρ of a soldered joint with temperature: *a* during heating; *b* during subsequent cooling (from [29])

per surfaces). The resistivity increases upon heating quite reversibly, although it decreases cycle by cycle, as shown by the results for three cycles of heating shown in Fig. 7.43. This change in resistivity relates to a change in thickness of the sandwich, as shown in Fig. 7.44. The thickness increases upon heating quite reversibly, decreasing cycle by cycle.

The thermal stability of the adhesive joint mentioned above can be improved by postcuring; i.e., by heating at an elevated temperature (e.g., 80°C for 4 h) after curing at room temperature (e.g., for 24 h). The postcuring removes the cycle-by-cycle decreases in resistivity (Fig. 7.43) and thickness (Fig. 7.44), meaning that the curves for various cycles essentially overlap.

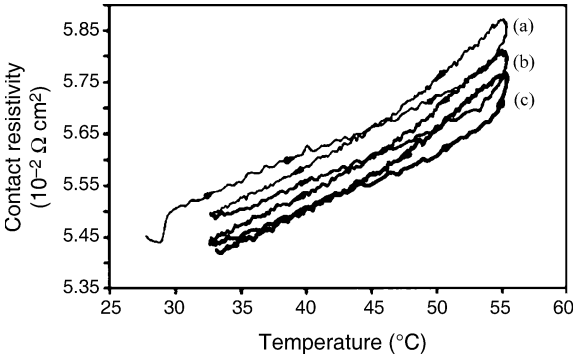

Figure 7.43. Contact electrical resistivity ϱ of an adhesive joint (silver epoxy between copper surfaces, without postcuring) during three cycles of heating at a constant compressive stress of 0.33 MPa. *a* First cycle, *b* second cycle, *c* third cycle. (From [30])

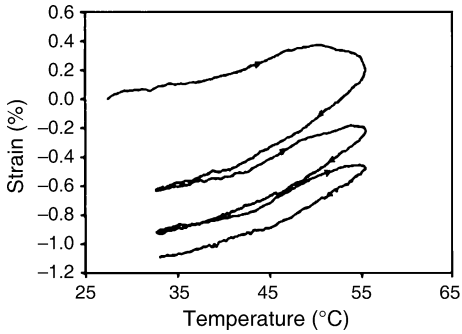

Figure 7.44. Strain (fractional change in sandwich thickness) of an adhesive joint (silver epoxy between copper surfaces, without postcuring) during three cycles of heating at a constant compressive stress of 0.33 MPa (from [30])

In some applications, the conductive adhesive needs to penetrate into a small space. Figure 7.45 shows the inability of silver epoxy (Product GPC-251, Creative Materials Inc., Tyngsboro, MA, USA, with 70–75 wt.% silver and bisphenol A epoxy resin, and a resistivity of 0.005 Ω cm after curing at 25°C) to penetrate into the small space between the 130 μm diameter strands of a seven-strand tin-coated copper wire. The electrical connection is between the wire and a substrate. This inadequate penetration is due to the high viscosity and hence low conformability of the silver epoxy. It causes a small area of contact between the silver epoxy and the wire, thus resulting in a high resistance at the interface between the silver epoxy and the wire. Figure 7.45 also shows that the silver flakes in the epoxy are about 15 μm in size and are preferentially oriented in the plane of the surfaces that are joined by the silver epoxy. The large dimensions of the silver flakes lead to the difficulties with the penetration of the silver epoxy into small spaces. In Fig. 7.45, one of the surfaces is the copper wire, the surface of which is curved. This preferred orientation of the silver flakes is not desirable, since it causes high resistance of the silver epoxy in the

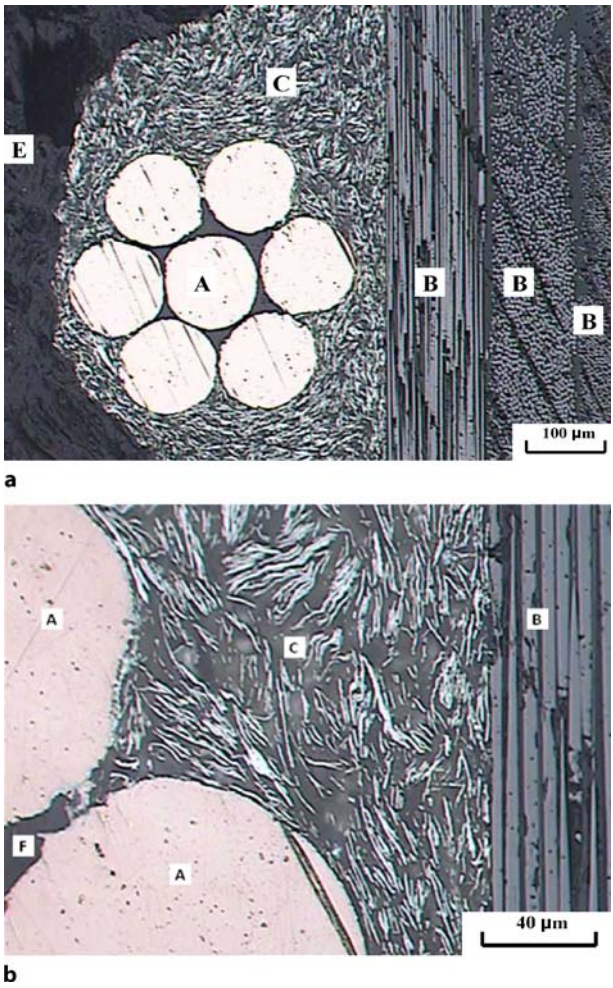

Figure 7.45. Optical microscope photographs of the cross-section of an electrical contact involving silver epoxy (a conductive adhesive). A – copper wire with seven strands; B – substrate in the form of a carbon fiber epoxy-matrix composite; C – silver epoxy, with the curved edges of the silver flakes shown; E – phenolic molding compound; *F*, void. **a** Low-magnification view, **b** high-magnification view. (From [31])

direction perpendicular to the plane of the joint, thereby increasing the resistance of the joint.

7.11.2 Mechanically Weak Joints for Electrical Conduction

An electrical connection does not have to be a strong mechanical joint, since the mechanical integrity can be derived from peripheral devices, such as clips and adhesive tape. By allowing the mechanical strength of the joint to be relatively weak, the choice of materials available is widened, thus allowing the electrical

resistance of the joint to minimized. For example, instead of an adhesive type of polymer (such as epoxy), numerous other organic vehicles can be used. Such conductive media are often known as conductive paints. A paint is a dispersion of fine conductive particles in a liquid, known as a vehicle. A common class of conductive paints uses volatile vehicles. A volatile vehicle evaporates from the joint interface after application, thereby allowing adjacent conductive particles in the paint to touch one another. In contrast, the polymer in a conductive adhesive is not volatile and remains at the interface between adjacent conductive particles, thus increasing the resistance of the particle–particle interface. In order to increase the ability of the paint to bond to a surface, a small proportion of a binder is typically used. The greater the proportion of binder, the stronger the bond mechanically, but the higher the electrical resistance of the bond. Therefore, it is necessary to make a compromise between the mechanical and electrical properties in the design of a conductive paint.

An example of a conductive paint is colloidal graphite, which is a dispersion of fine graphite particles in water (a volatile vehicle). Polyvinyl alcohol (PVA), which dissolves in water, is a commonly used binder for water-based dispersions. Another example is silver paint, which is a dispersion of silver particles in a volatile vehicle, such as propanol (an alcohol). Ethyl cellulose (the ethyl ether of cellulose) is a commonly used binder for organic-based dispersions, as it is soluble in some organic solvents (e.g., ethanol), though it is insoluble in water. The solubility in organics depends on the ethoxyl ($-OC_2H_5$) content in the particular ethyl cellulose.

Figure 7.46 shows that silver paint (Product Electrodag 416, from Acheson Colloids Co., Port Huron, MI, USA, consisting of 45 wt.% silver particles, 1–5 wt.% ethyl cellulose, which is a binder, and 48 wt.% ethanol, which is the volatile vehicle, with a resistivity of 0.003 Ω cm) is able to penetrate into small spaces due to its low viscosity. The silver particles in the paint are so small that they are not individually observed in the optical micrograph, in contrast to the large size of the silver flakes in the silver epoxy of Fig. 7.45.

Figure 7.47 shows that graphite colloid (LUBRODAL EC 1204 B, from Fuchs Lubricant Co., Emlenton, PA, USA, a water-based dispersion containing less than 20 wt.% graphite particles of size $< 0.75\,\mu m$, less than 1 wt.% sodium salt of cellulose, which is a binder, and less than 1 wt.% dispersants, with a resistivity of 0.03–0.10 Ω cm, which is much higher than that of the silver paint mentioned above) is able to penetrate into small spaces due to its low viscosity. The graphite particles in the paint are so small that they are not individually observed in the optical micrograph. Graphite colloid is much less expensive than silver paint.

Comparing the silver epoxy (Fig. 7.45), silver paint (Fig. 7.46) and graphite colloid (Fig. 7.47) mentioned above shows that the resistance of the electrical contact between the copper wire and the substrate is lowest for silver paint and is relatively high for graphite colloid and silver epoxy. The silver epoxy joint degrades under hydrothermal conditions (40°C in water for 60 min), meaning that the resistance increases further. This is because of the low hygrothermal stability of epoxy. In contrast, silver paint degrades only slightly under the same conditions. Graphite colloid degrades even more significantly than silver epoxy due to the fact that it is water based.

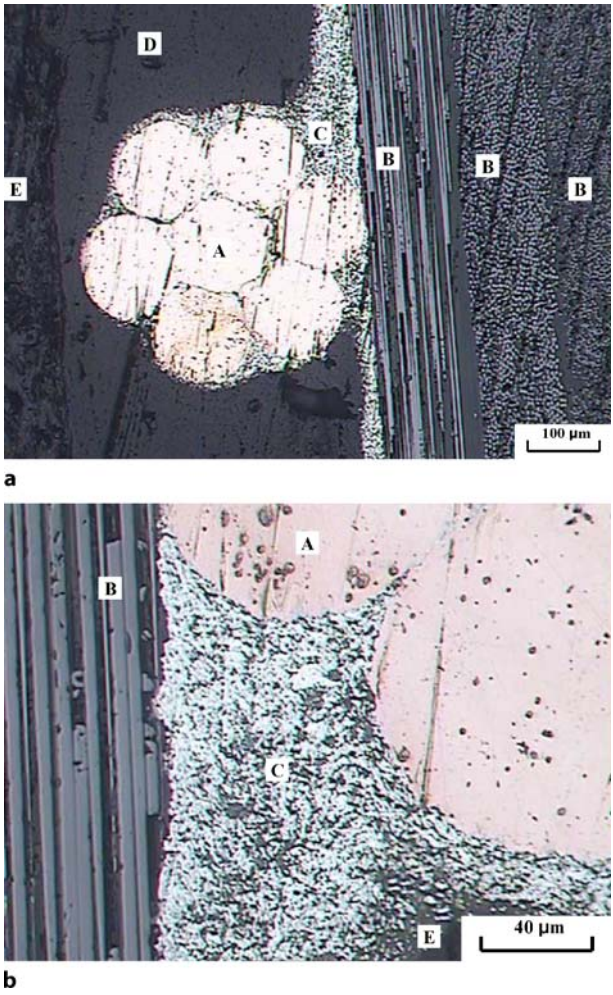

Figure 7.46. Optical microscope photographs of the cross-section of an electrical contact involving silver paint. A – copper wire with seven strands; B – substrate in the form of a carbon fiber epoxy-matrix composite; C – silver paint; D – epoxy overcoat; E – phenolic molding compound. **a** Low-magnification view, **b** high-magnification view. (From [31])

The combined use of silver particles and a low proportion of carbon black (0.055 of the total filler volume) provides a paint that performs well both electrically and mechanically [32]. Carbon black is less conductive than silver by a few orders of magnitude. However, it is inexpensive and is used in the form of porous agglomerates of nanoparticles. This morphology allows carbon black to be highly compressible (squishable), meaning that it is highly conformable. Because of this conformability, the carbon black fills the space among the silver particles, thereby improving both the electrical conductivity and the scratch resistance of the resulting conductive film. The scratch resistance relates to the shear strength of the film. With a total solid volume fraction of 0.1969 and a silane-propanol (1:1 by weight)

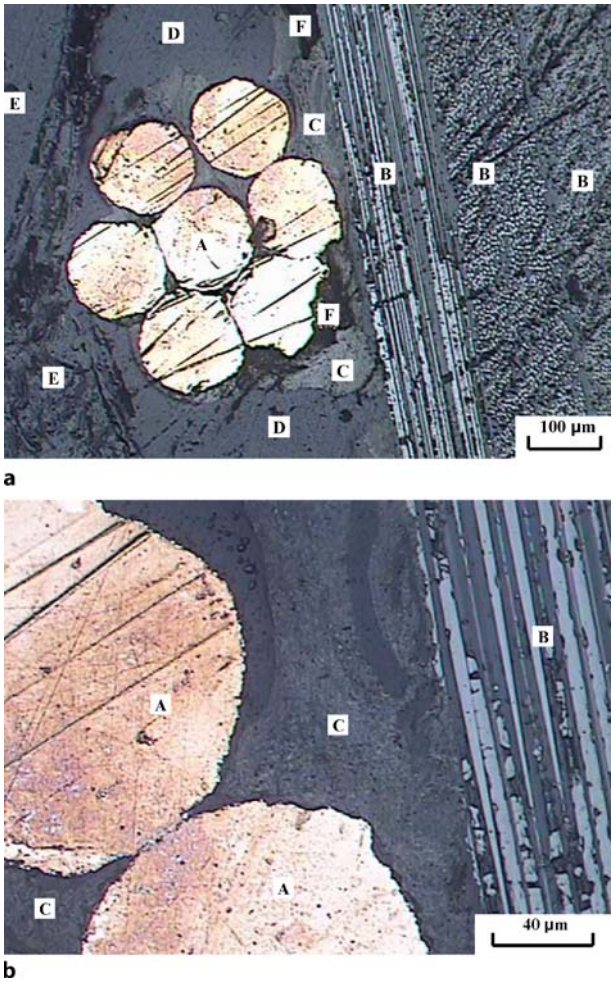

Figure 7.47. Optical microscope photographs of the cross-section of an electrical contact involving graphite colloid. A – copper wire with seven strands; B – substrate in the form of a carbon fiber epoxy-matrix composite; C – graphite colloid; D – epoxy overcoat; E – phenolic molding compound; F – void. **a** Low-magnification view, **b** high-magnification view. (From [31])

solution vehicle, a conductive film of resistivity $2 \times 10^{-3}\,\Omega\,\mathrm{cm}$ (in the plane of the film) and thickness 50 µm is obtained. The combined use of silane and propanol in the vehicle is due to the hydrolysis of silane with the aqueous propanol solution and the mechanical strengths of the resulting reaction products.

7.11.3 Electrical Connection Through Pressure Application

An electrical connection that requires continuous pressure application in order for it to function is known as a pressure contact. Although the requirement for pressure is a disadvantage, pressure contacts are attractive since they are separable

connections. A connection involving a clip is an example of a pressure contact; here, connecting and disconnecting simply involve clipping and unclipping. In contrast, disconnection is not as simple for a joint involving solder or adhesive. A pressure contact should be distinguished from conductive adhesive, conductive paint and solder connections, which tend to degrade upon the application of pressure.

Positioning a material at the pressure contact interface can help to improve the contact, particularly if it is conformable to the surface topography of the adjoining surfaces. Surfaces are never perfectly smooth; they have microscopic hillocks. The valley between two hillocks contains air, which is an insulator. Therefore, the conformability of the material enables the displacement of air from the contact interface, thereby decreasing the electrical resistance of the interface.

Due to the conformability of carbon black, carbon black paste makes a particularly effective pressure contact interface material [33]. It yields a contact resistivity of $2 \times 10^{-5}\,\Omega\,\mathrm{cm}^2$ in the direction perpendicular to the plane of the contact when the contact pressure is 0.92 MPa, compared to the higher value of $1 \times 10^{-4}\,\Omega\,\mathrm{cm}^2$ for a pressure contact without an interface material.

7.11.4 Electrical Connection Through a *Z*-Axis Electrical Conductor

A *z*-axis anisotropic electrical conductor is a conducting sheet that conducts only in the *z*-direction, which is the direction perpendicular to the sheet. It is insulating in all other directions. Such a conductor is a composite material involving an insulating matrix and conductive columns that are perpendicular to the plane of the sheet, as illustrated in Fig. 7.48. Since the columns do not touch one another, the sheet is insulating in the plane of the sheet. The columns do not need to be regularly spaced.

The presence of a polymer matrix film, which is insulating, on the conductive column surface in the plane of the sheet must be avoided. To ensure this, each column protrudes slightly from each of the two outer surfaces of the sheet in one of the designs.

Z-axis conductors are used for electrically connecting corresponding contact pads on the two proximate surfaces that sandwich the *z*-axis conductor. One or more conductive columns can link a pair of contact pads on each surface, as shown in Fig. 7.48. If the column density is high enough that there is at least one conductive column per pair of opposite contact pads, there is no need to align

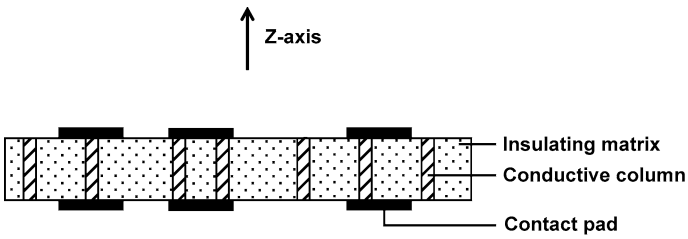

Figure 7.48. A *z*-axis anisotropic electrical conductor

the *z*-axis conductor sheet relative to the two proximate surfaces. However, if the column density is low and/or the contact pad size is small, alignment is necessary and, in this case, the columns are regularly spaced.

A single sheet of a *z*-axis conductor can replace a two-dimensional array of soldered joints. It is thus attractive for replacing solder and reducing processing costs. The *z*-axis conductor can take the form of a standalone sheet or an adhesive. The standalone sheet needs to be squeezed between the proximate surfaces by fastening. The adhesive becomes a *z*-axis conductor sheet after application and does not require fastening.

Each conductive column can take the form of a single conductive particle (which is not necessarily columnar in shape, but must be large enough to extend for the entire thickness of the sheet), a cluster (or column) of conductive particles, or a single wire that is oriented along the *z*-axis. A single particle is advantageous compared to a cluster of particles, due to the presence of contact resistance at the interface between particles in a cluster. For a standalone sheet, all of these options are possible, due to the variety of methods available for introducing and orienting the conductive component in a composite sheet. For example, the orientation of a particle column or a wire can be achieved through the use of an electric or magnetic field. For an adhesive, the single particle option is typically used, since orientation is difficult after the application of the particle-filled adhesive at the joint interface. In other words, the single particles are randomly distributed in the adhesive after application to the joint interface, with the particles not in contact with one another.

The conductive particles in a *z*-axis conductor involving a single particle per conductive column must have a narrow size distribution. Otherwise, the particles that are small cannot extend for the entire thickness of the sheet and thus cannot serve as a conductive column. Ideally, all of the particles are slightly larger than the thickness of the sheet.

The conductive particles used in a *z*-axis conductor can be metal particles or metal-coated polymer particles. The latter is attractive due to the ease with which the particles can be deformed in response to the fastening stress. A limited degree of erosion of the metal coating on a polymer particle is acceptable, although, in the case of a single particle per column, the fragmented coating must extend for the entire thickness of the sheet. However, the latter is disadvantageous due to the small volume of metal in a metal-coated polymer particle and the consequent high resistance of a conductive column compared to a metal particle.

7.12 Porous Conductors

Porous conductors are important for electrodes and current collectors in electrochemical devices such as batteries, in addition to applications related to filters and catalyst supports. For the abovementioned applications (other than catalyst supports), the pores need to be continuous and accessible from the outer surface so that fluids can flow in the porous conductor. The porosity (i.e., the fraction of

the volume occupied by pores) is typically high, exceeding 50%. Pores are generally detrimental to mechanical properties. The larger the pore size, the lower the strength. However, mechanical strength and modulus are typically not needed for electrochemical applications.

A porous conductor can take the form of a collection of conductive particles or fibers. In order to provide some mechanical integrity, a small amount of binder may be used with the conductive particles or fibers. In some electrochemical electrodes, the active component is not conductive, as in the case of manganese dioxide particles used as a cathode material, so conductivity is achieved by using a conductive additive, which can be conductive particles or fibers that are mixed with the active component.

One method of making porous conductors involves dry compaction of a collection of conductive particles or short fibers, optionally in the presence of a small amount of a binder, which is typically a thermoplastic polymer powder. The binder flows upon heating, thereby providing binding. Examples of thermoplastic binders are polytetrafluoroethylene (Teflon) and polyvinylidene fluoride (PVDF). By varying the pressure used for compacting, different volume fractions of the filler may be obtained.

Another method of making porous conductors involves (i) making a slurry of the conductive particles or short fibers dispersed in a liquid, (ii) casting the slurry and then baking to remove the liquid, thereby forming a preform, (iii) infiltrating the preform with a binder, and (iv) heating to cause the binder to bind.

A binder may be conductive or nonconductive. A polymer binder is nonconductive. A conductive binder is obviously attractive for making a porous conductor. An example of a conductive binder is carbon, which is made from a carbon precursor, such as pitch, by carbonization (heating). The pitch may be used in the molten state. Alternatively, it may be used at room temperature by dissolving it in a solvent, such as methylene chloride. With carbon fiber used as the conductive filler and a carbon binder, the resulting porous conductor is all carbon and is thus attractive due to its chemical resistance, high temperature resistance, thermal conductivity, and low CTE.

7.12.1 Porous Conductors Without a Nonconductive Filler

A low resistivity of the filler is obviously advantageous for providing a low resistivity in the resulting porous conductor. Thus, graphitized carbon nanofiber is more effective than carbon nanofiber that has not been graphitized. The resistivities of a carbon nanofiber (0.1 μm diameter) compact without a binder are 0.053 and 0.0095 Ω cm for nongraphitized and graphitized carbon nanofibers, respectively, where the density of the porous carbon is 0.47 g/cm^3 in both cases (compared to a density of 2 g/cm^3 for the nanofiber itself) [34].

The contact resistance at a filler–filler contact point in a porous conductor is comparable to that in a polymer-matrix composite with the same filler at a similar volume fraction. This is indicated by the similarity in the volume resistivity. For example, the volume resistivity is 4.1×10^{-2} Ω cm for a carbon nanofiber (0.1

μm diameter, not graphitized) compact without a binder and with a nanofiber content of 28%, compared to a resistivity of $6.2 \times 10^{-2}\,\Omega\,\mathrm{cm}$ for a dense carbon nanofiber (0.1 μm diameter, not graphitized) polyethersulfone-matrix composite with a nanofiber content of 25% [35].

A high aspect ratio of the filler is also advantageous because of the smaller number of filler–filler contact points. The resistivity of a carbon nanofiber (0.05 μm diameter, with aspect ratio 20–50) compact without a binder is $0.21\,\Omega\,\mathrm{cm}$ at a density of $0.49\,\mathrm{g/cm^3}$, compared to a low value of $0.053\,\Omega\,\mathrm{cm}$ at a density of $0.47\,\mathrm{g/cm^3}$ for the carbon nanofiber (0.1 μm diameter, with aspect ratio 50–200) mentioned above [34]. Furthermore, a conductive filler in the form of particles (e.g., carbon black) is less effective than one in the form of fibers (e.g., carbon nanofiber) at providing a porous material of low resistivity.

In the case of a porous carbon with a discontinuous carbon fiber, the length of the fiber matters greatly. As shown for a carbon matrix (with pitch as the precursor), the longer the fiber, the higher (i) the mean pore size, (ii) the specific geometric surface area (surface area per unit volume), (iii) the porosity, and (iv) the resistivity of the resulting porous carbon [36].

7.12.2 Porous Conductors With a Nonconductive Filler and a Conductive Additive

In the presence of a nonconductive filler, which provides the necessary function for the porous conductor, a conductive additive is necessary. Only a small amount of the conductive additive is applied, but it needs to provide a continuous conductive path. Carbon black is even more effective than carbon nanofiber as a conductive additive because of its squishability, which stems from its presence in the form of porous agglomerates of nanoparticles, and which facilitates the formation of a continuous conductive path. The carbon black is squished between adjacent nonconductive filler particles (60 μm manganese dioxide particles) during the compaction. This contrasts sharply with the case where the nonconductive filler is absent (Sect. 7.11.1). In the absence of a nonconductive filler, the squishability of the conductive filler is much less important.

An increase in the amount of binder can increase or decrease the resistivity of a porous conductor, depending on the particular conductive filler used. This has been shown when manganese dioxide particles (60 μm) were used as the nonconductive filler and PVDF (5 μm particles) as the binder [37]. When carbon black (0.05 μm particles), which is squishable, is used as the conductive additive, decreasing the amount of binder from 10 to 6 wt.% decreases the resistivity slightly. However, when the conductive additive is natural graphite powder (27 μm particles), the resistivity increases greatly when the binder amount is decreased. This is attributed to the positive influence of the binder on the conductive additive dispersion when the filler is not squishable. The lower the degree of conductive additive dispersion, the higher the resistivity of the porous conductor. In other words, a particulate filler that is not squishable needs the binder to aid its dispersion. When the conductive additive is carbon nanofibers (0.1 μm diameter), which

are not squishable but have high aspect ratios, decreasing the amount of binder results in a moderate increase in the resistivity.

Review Questions

1. Why is graphite a good electrical conductor in the planes of the carbon layers, but a poor electrical conductor perpendicular to the layers?
2. Why does the electrical resistivity of a metal increase with increasing temperature?
3. Why does the contact electrical resistivity of the interlaminar interface of a carbon fiber (continuous) epoxy-matrix composite decrease with increasing temperature?
4. Why is a conductor with an electrical resistance that is too high ineffective for resistance heating?
5. Why is a metal typically a poor thermoelectric material (i.e., one with a low value of ZT)?
6. Why is a polymer typically a poor thermoelectric material (i.e., one with a low value of ZT)?
7. Which parts of an electronic package can benefit from using a metal-matrix composite with a low thermal expansion and high thermal conductivity?
8. What is the function of glass frit (i.e., glass particles) in a thick-film electrical conductor paste?
9. Describe a process for making a multilayer ceramic chip carrier.
10. What is the main application of a z-axis conductor film?
11. Thermally conducting but electrically insulating polymer-matrix composites are useful for which aspects of electronic packaging?
12. Give an example of each of the following:
    a. A z-axis conductor
    b. An electrically conductive thick-film paste.
13. The following materials are used in electronic packaging. For each material, describe the properties that make it useful for electronic packaging.
    a. Kovar
    b. Silver-epoxy
    c. BN-epoxy.
14. What is the main advantage of a surface-mounting type of electronic package compared to a pin-inserting type of package?
15. What are the three main ingredients of a printed circuit board?

16. What are the two attractive properties of metal-matrix composites that make them useful for electronic packaging applications?
17. Why are ceramics that can be sintered at temperatures of below 1,000°C attractive for electronic packaging?
18. What are the two main problems with soldered joints in an electronic package?
19. What are the two main criteria that govern the effectiveness of a *z*-axis conductor?

References

[1] S. Wang, S. Wen and D.D.L. Chung, "Resistance Heating Using Electrically Conductive Cements", *Adv. Cem. Res.* 16(4), 161–166 (2004).

[2] A. Fosbury, S. Wang, Y.F. Pin and D.D.L. Chung, "The Interlaminar Interface of a Carbon Fiber Polymer-Matrix Composite as a Resistance Heating Element", *Compos. Part A* 34, 933–940 (2003).

[3] S. Wang, D.P. Kowalik and D.D.L. Chung, "Self-Sensing Attained in Carbon Fiber Polymer-Matrix Structural Composites by Using the Interlaminar Interface as a Sensor", *Smart Mater. Struct.* 13(3), 570–592 (2004).

[4] S. Wen and D.D.L. Chung, "Carbon Fiber-Reinforced Cement as a Thermistor," *Cem. Concr. Res.* 29(6), 961–965 (1999).

[5] J. Cao and D.D.L. Chung, "Damage Evolution During Freeze-Thaw Cycling of Cement Mortar, Studied by Electrical Resistivity Measurement", *Cem. Concr. Res.* 32(10), 1657–1661 (2002).

[6] X. Wang and D.D.L. Chung, "Self-Monitoring of Fatigue Damage and Dynamic Strain in Carbon Fiber Polymer-Matrix Composite," *Compos. Part B* 29(1), 63–73 (1998).

[7] S. Wang, D.D.L. Chung and J.H. Chung, "Impact Damage of Carbon Fiber Polymer-Matrix Composites, Monitored by Electrical Resistance Measurement", *Compos. Part A* 36, 1707–1715 (2005).

[8] S. Wang and D.D.L. Chung, "Self-Sensing of Flexural Strain and Damage in Carbon Fiber Polymer-Matrix Composite by Electrical Resistance Measurement", *Carbon* 44(13), 2739–2751 (2006).

[9] D. Wang and D.D.L. Chung, "Through-Thickness Stress Sensing of Carbon Fiber Polymer-Matrix Composite by Electrical Resistance Measurement", *Smart Mater. Struct.* 16, 1320–1330 (2007).

[10] S. Wang and D.D.L. Chung, "The Interlaminar Interface of a Carbon Fiber Epoxy-Matrix Composite as an Impact Sensor", *J. Mater. Sci.* 40, 1863–1867 (2005).

[11] S. Wen and D.D.L. Chung, "Strain Sensing Characteristics of Carbon Fiber Reinforced Cement", *ACI Mater. J.* 102(4), 244–248 (2005).

[12] S. Zhu and D.D.L. Chung, "Theory of Piezoresistivity for Strain Sensing in Carbon Fiber Reinforced Cement Under Flexure", *J. Mater. Sci.* 42(15), 6222–6233 (2007).

[13] S. Wen and D.D.L Chung, "Self-Sensing of Flexural Damage and Strain in Carbon Fiber Reinforced Cement and Effect of Embedded Steel Reinforcing Bars", *Carbon* 44(8), 1496–1502 (2006).

[14] G.J. Snyder, E.C. Toberer, "Complex Thermoelectric Materials", *Nature Mater.* 7, 105 (2008).

[15] T.M. Tritt, H. Boettner, L. Chen, "Thermodynamics: Direct Solar Thermal Energy Conversion", *MRS Bull.* 33, 366 (2008).

[16] B. Poudel, Q. Hao, Y. Ma, Y. Lan, A. Minnich, B. Yu, X. Yan, D. Wang, A. Muto, D. Yashaee, X. Chen, J. Liu, M.S. Dresselhaus, G. Chen, Z. Ren, "High-Thermoelectric Performance of Nanostructured Bismuth Antimony Telluride Bulk Alloys", *Science* 320, 634 (2008).

[17] R. Venkatasubramanian, E. Siivola, T. Colpitts, B. O'Quinn, "Thin-Film Thermoelectric Devices with High Room-Temperature Figure of Merit", *Nature* 413, 597 (2001).

[18] H. Ohta, S. Kim, Y. Mune, T. Mizoguchi, K. Nomura, S. Ohta, T. Nomura, Y. Nakanishi, Y. Ikuhara, M. Hirano, H. Hosono, K. Koumoto, "Giant Thermoelectric Seebeck Coefficient of a Two-Dimensional Electron Gas in $SrTiO_3$", *Nat. Mater.* 6, 129 (2007).

[19] O. Yamashita, H. Odahara, "Effect of the Thickness of Bi-Te Compound and Cu Electrode on the Resultant Seebeck Coefficient in Touching Cu/Bi-Te/Cu Composites", *J. Mater. Sci.* 42, 5057 (2007).

[20] O. Yamashita, K. Satou, H. Odahara, S. Tomiyoshi, "Enhancement of the Thermoelectric Figure of Merit in $M/T/M$ (M = Cu or Ni and $T = Bi_{0.88}Sb_{0.12}$) Composite Materials" *J. Appl. Phys.* 98, 073707 (2005).
[21] V. H. Guerrero, S. Wang, S. Wen, D.D.L. Chung, "Thermoelectric Property Tailoring by Composite Engineering", *J. Mater. Sci.* 37(19), 4127–4136 (2002).
[22] S. Han, S. Wang, D.D.L. Chung, *SAMPE Fall Tech. Conf.*, 2009. [9]
[23] G.-D. Zhan, J.D. Kuntz, A.K. Mukherjee, P. Zhu, K. Koumoto, "Thermoelectric Properties of Carbon Nanotube/Ceramic Nanocomposites", *Scr. Mater.* 54, 77 (2006).
[24] X. Shui and D.D.L. Chung, "Submicron Diameter Nickel Filaments and Their Polymer-Matrix Composites", *J. Mater. Sci.* 35, 1773–1785 (2000).
[25] L. Li and D.D.L. Chung, "Effect of Viscosity on the Electrical Properties of Conducting Thermoplastic Composites Made by Compression Molding of a Powder Mixture", *Polym. Compos.* 14(6), 467–472 (1993).
[26] L. Li and D.D.L. Chung, "Electrically Conducting Powder Filled Polyimidesiloxane", *Composites* 22(3), 211–218 (1991).
[27] P.-W. Chen, X. Fu, and D.D.L. Chung, "Microstructural and Mechanical Effects of Latex, Methylcellulose and Silica Fume on Carbon Fiber Reinforced Cement", *ACI Mater. J.* 94(2), 147–155 (1997).
[28] K.-D. Kim and D.D.L. Chung, "Electrically Conductive Adhesive and Soldered Joints under Compression", *J. Sci. Tech.* 19(11), 1003–1023 (2005).
[29] K.-D. Kim and D.D.L. Chung, "Effect of Heating on the Electrical Resistivity of Conductive Adhesive and Soldered Joints", *J. Electron. Mater.* 31(9), 933–939 (2002).
[30] J. Xiao and D.D.L. Chung, "Thermal and Mechanical Stability of Electrical Conductive Adhesive Joints", *J. Electron. Mater.* 34(5), 625–629 (2005).
[31] S. Wang, D.S. Pang and D.D.L. Chung, "Hygrothermal Stability of Electrical Contacts Made from Silver and Graphite Electrically Conductive Pastes", *J. Electron. Mater.* 36(1), 65–74 (2007).
[32] C.-K. Leong and D.D.L. Chung, "Improving the Electrical and Mechanical Behavior of Electrically Conductive Paint by Partial Replacement of Silver by Carbon Black", *J. Electron. Mater.* 35(1), 118–122 (2006).
[33] C.-K. Leong and D.D.L. Chung, "Pressure Electrical Contact Improved by Carbon Black Paste", *J. Electron. Mater.* 33(3), 203–206 (2004).
[34] X. Shui and D.D.L. Chung, "Electrical Resistivity of Submicron-Diameter Carbon-Filament Compacts", *Carbon* 39 (ER11), 1717–1722 (2001).
[35] D.D.L. Chung, "Comparison of Submicron Diameter Carbon Filaments and Conventional Carbon Fibers as Fillers in Composite Materials", *Carbon* 39(8), 1119–1125 (2001).
[36] X. Shui and D.D.L. Chung, "High-Strength High-Surface-Area Porous Carbon Made From Submicron-Diameter Carbon Filaments," *Carbon* 34(6), 811–814 (1996); 34(9), 1162 (1996).
[37] W. Lu and D.D.L. Chung, "A Comparative Study of Carbons for Use as an Electrically Conducting Additive in the Manganese Dioxide Cathode of an Electrochemical Cell", *Carbon* 40 (ER3), 447–449 (2002).

Further Reading

J. Cao and D.D.L. Chung, "Microstructural Effect of the Shrinkage of Cement-Based Materials During Hydration, as Indicated by Electrical Resistivity Measurement", *Cem. Concr. Res.* 34(10), 1893–1897 (2004).
D.D.L. Chung, "Electrical Behavior of Solids," *J. Educ. Mod. Mat. Sci. Eng.* 2, 747 (1980).
D.D.L. Chung, "Thermal Analysis of Carbon Fiber Polymer-Matrix Composites by Electrical Resistance Measurement", *Thermochim. Acta* 364, 121–132 (2000).
D.D.L. Chung, "Continuous Carbon Fiber Polymer-Matrix Composites and Their Joints, Studied by Electrical Measurements", *Polym. Compos.* 22(2), 250–270 (2001).
D.D.L. Chung, "Thermal Analysis by Electrical Resistivity Measurement", *J. Therm. Anal. Calorim.* 65, 153–165 (2001).

D.D.L. Chung, "Piezoresistive Cement-Based Materials for Strain Sensing", *J. Intell. Mater Syst. Struct.* 13(9), 599–609 (2002).
D.D.L. Chung, "Damage in Cement-Based Materials, Studied by Electrical Resistance Measurement", *Mater. Sci. Eng. R* 42(1), 1–40 (2003).
D.D.L. Chung, "Self-Heating Structural Materials", *Smart Mater. Struct.* 13(3), 562–565 (2004).
D.D.L. Chung, "Electrically Conductive Cement-Based Materials", Adv. Cem. Res. 16(4), 167–176 (2004).
D.D.L. Chung, "Electrical Applications of Carbon Materials", *J. Mater. Sci.* 39(8), 2645–2661 (2004).
D.D.L. Chung, "Dispersion of Short Fibers in Cement", *J. Mater. Civil Eng.* 17(4), 379–383 (2005).
D.D.L. Chung, "Damage Detection Using Self-Sensing Concepts" (Invited Review), *J. Aerosp. Eng. (Proc. Inst. Mech. Eng., Part G)* 221(G4), 509–520 (2007).
V.H. Guerrero, S. Wang, S. Wen and D.D.L. Chung, "Thermoelectric Property Tailoring by Composite Engineering", *J. Mater. Sci.* 37(19), 4127–4136 (2002).
D. Wang and D.D.L. Chung, "Through-Thickness Stress Sensing of Carbon Fiber Polymer-Matrix Composite by Electrical Resistance Measurement", *Smart Mater. Struct.* 16, 1320–1330 (2007).
S. Wang and D.D.L. Chung, "The Interlaminar Interface of a Carbon Fiber Epoxy-Matrix Composite as an Impact Sensor", *J. Mater. Sci.* 40, 1863–1867 (2005).
S. Wang and D.D.L. Chung, "Negative Piezoresistivity in Continuous Carbon Fiber Epoxy-Matrix Composite", *J. Mater. Sci.* 42(13), 4987–4995 (2007).
S. Wen and D.D.L. Chung, "Strain Sensing Characteristics of Carbon Fiber Reinforced Cement", *ACI Mater. J.* 102(4), 244–248 (2005).
S. Wen and D.D.L. Chung, "Spatially Resolved Self-Sensing of Strain and Damage in Carbon Fiber Cement", *J. Mater. Sci.* 41(15), 4823–4831 (2006).
S. Wen and D.D.L. Chung, "Model of Piezoresistivity in Carbon Fiber Cement", *Cem. Concr. Res.* 36(10), 1879–1885 (2006).
S. Wen and D.D.L. Chung, "Double Percolation in the Electrical Conduction in Carbon Fiber Reinforced Cement-Based Materials", *Carbon* 45(2), 263–267 (2007).
S. Wen and D.D.L. Chung, "Electrical-Resistance-Based Damage Self-Sensing in Carbon Fiber Reinforced Cement", *Carbon* 45(4), 710–716 (2007).
S. Wen and D.D.L. Chung, "Piezoresistivity-Based Strain Sensing in Carbon Fiber Reinforced Cement", *ACI Mater. J.* 104(2), 171–179 (2007).
D.C. Wobschall and D.D.L. Chung, "Ohmmeters", *The Encyclopedia of Electrical and Electronics Engineering*, Wiley, New York, 1999, vol. 15, pp. 122–123.
S. Zhu and D.D.L. Chung, "Analytical Model of Piezoresistivity for Strain Sensing in Carbon Fiber Polymer-Matrix Structural Composite under Flexure", *Carbon* 45(8), 1606–1613 (2007).
S. Zhu and D.D.L. Chung, "Theory of Piezoresistivity for Strain Sensing in Carbon Fiber Reinforced Cement Under Flexure", *J. Mater. Sci.* 42(15), 6222–6233 (2007).
S. Zhu and D.D.L. Chung, "Numerical Assessment of the Methods of Measurement of the Electrical Resistance in Carbon Fiber Reinforced Cement", *Smart Mater. Struct.* 16, 1164–1170 (2007).